AD-A055 759 SYRACUSE UNIV NY DEPT OF ELECTRICAL AND COMPUTER SCIENCE F/G 9/5
METHOD OF MOMENT THIN WIRE COMPUTER PROGRAM COMPARISONS FOR COM--ETC(U)
MAY 78 J PERINI, H K SCHUMAN F30602-75-C-0121

UNCLASSIFIED RADC-TR-78-106 NL

| OF |
ADA
055759

END
DATE
FILMED
8-78
DDC

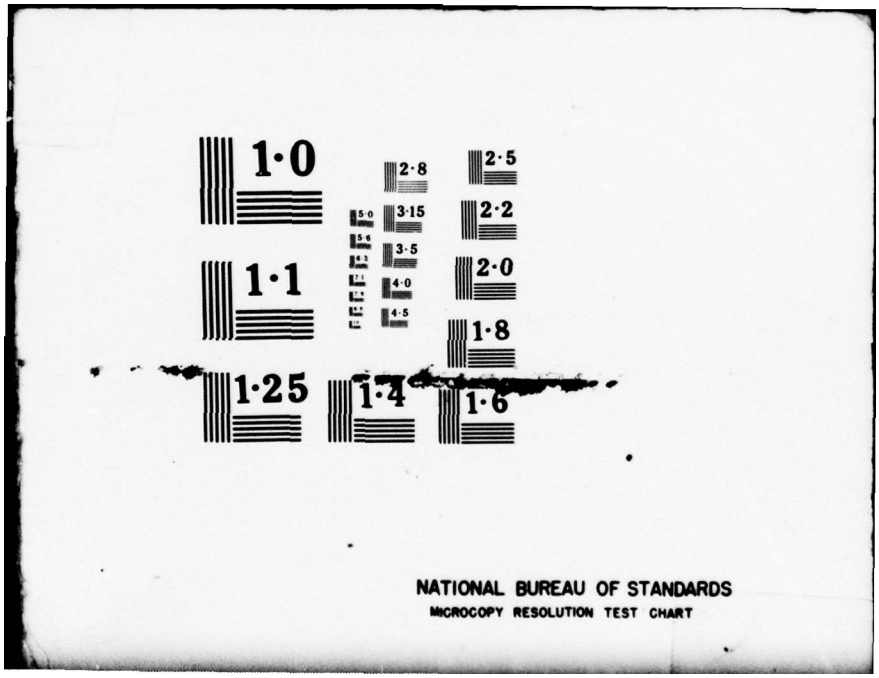
1·0
1·1
1·25
2·8
3·15
3·5
4·0
4·5
5·0
2·5
2·2
2·0
1·8
1·4
1·6
NATIONAL BUREAU OF STANDARDS
MICROCOPY RESOLUTION TEST CHART

RADC-TR-78-106
Phase Report
May 1978

METHOD OF MOMENT THIN WIRE COMPUTER PROGRAM COMPARISONS FOR COMPLEX STRUCTURES AND COARSE ACCURACY

Dr. Jose Perini
Dr. Harvey K. Schuman

Syracuse University

ROME AIR DEVELOPMENT CENTER
Air Force Systems Command
Griffiss Air Force Base, New York 13441

This report has been reviewed by the RADC Information Office (OI) and is releasable to the National Technical Information Service (NTIS). At NTIS it will be releasable to the general public, including foreign nations.

RADC-TR-78-106 has been reviewed and is approved for publication.

APPROVED: Jacob Scherer

JACOB SCHERER
Project Engineer

APPROVED: Joseph J. Naresky

JOSEPH J. NARESKY
Chief, Reliability & Compatibility Division

FOR THE COMMANDER: John P. Huss

JOHN P. HUSS
Acting Chief, Plans Office

If your address has changed or if you wish to be removed from the RADC mailing list, or if the addressee is no longer employed by your organization, please notify RADC (RBC) Griffiss AFB NY 13441. This will assist us in maintaining a current mailing list.

Do not return this copy. Retain or destroy.

UNCLASSIFIED

SECURITY CLASSIFICATION OF THIS PAGE *(When Data Entered)*

REPORT DOCUMENTATION PAGE

READ INSTRUCTIONS BEFORE COMPLETING FORM

1. REPORT NUMBER: RADC-TR-78-106	2. GOVT ACCESSION NO.
3. RECIPIENT'S CATALOG NUMBER	
4. TITLE (and Subtitle): METHOD OF MOMENT THIN WIRE COMPUTER PROGRAM COMPARISONS FOR COMPLEX STRUCTURES AND COARSE ACCURACY.	5. TYPE OF REPORT & PERIOD COVERED: Phase Report.
	6. PERFORMING ORG. REPORT NUMBER
7. AUTHOR(s): Dr. Jose Perini; Dr. Harvey K. Schuman	8. CONTRACT OR GRANT NUMBER(s): F30602-75-C-0121
9. PERFORMING ORGANIZATION NAME AND ADDRESS: Syracuse University, Syracuse NY 13210	10. PROGRAM ELEMENT, PROJECT, TASK AREA & WORK UNIT NUMBERS: 920W, 95670016
11. CONTROLLING OFFICE NAME AND ADDRESS: Rome Air Development Center (RBC), Griffiss AFB NY 13441	12. REPORT DATE: May 1978
	13. NUMBER OF PAGES: 72 (12) 79 p.
14. MONITORING AGENCY NAME & ADDRESS *(if different from Controlling Office)*: Same (16) 9567	15. SECURITY CLASS. *(of this report)*: UNCLASSIFIED
	15a. DECLASSIFICATION/DOWNGRADING SCHEDULE: N/A

16. DISTRIBUTION STATEMENT *(of this Report)* (17) 00

Approved for public release; distribution unlimited.

17. DISTRIBUTION STATEMENT *(of the abstract entered in Block 20, if different from Report)*

Same

18. SUPPLEMENTARY NOTES

Project Engineer: Jacob Scherer (RBC)

19. KEY WORDS *(Continue on reverse side if necessary and identify by block number)*

Antennas
Method of Moments Analysis

20. ABSTRACT *(Continue on reverse side if necessary and identify by block number)*

Three typical thin-wire moment method computer programs OS (sinusoidal Galerkin) SYR (triangle Galerkin), and WRSMOM (pulse expansion-impulse weighting) are compared. They are applied to four antenna models -- two simple and two complex. The complex models are representative of shipboard "twin fan" antennas. The primary purpose is to determine if a "best" computer program exists given "coarse" accuracy (within ±3 dB of converged results) as acceptable in predicting the driving point impedances and farfield radiation patterns exhibited by

DD FORM 1 JAN 73 1473 EDITION OF 1 NOV 65 IS OBSOLETE

UNCLASSIFIED

SECURITY CLASSIFICATION OF THIS PAGE *(When Data Entered)*

PREFACE

This effort was conducted by Syracuse University under the sponsorship of the Rome Air Development Center Post-Doctoral Program for the Navy. Mr. Tony Testa of NAVSEC was the task project engineer and provided overall technical direction and guidance. The authors of this report are Dr. Jose Perini and Dr. Harvey Schuman.

The RADC Post-Doctoral Program is a cooperative venture between RADC and some sixty-five universities eligible to participate in the program. Syracuse University (Department of Electrical and Computer Engineering), Purdue University (School of Electrical Engineering), Georgia Institute of Technology (School of Electrical Engineering), and State University of New York at Buffalo (Department of Electrical Engineering) act as prime contractor schools with other schools participating via sub-contracts with the prime schools. The U.S. Air Force Academy (Department of Electrical Engineering), Air Force Institute of Technology (Department of Electrical Engineering), and the Naval Post Graduate School (Department of Electrical Engineering) also participate in the program.

The Post-Doctoral Program provides an opportunity for faculty at participating universities to spend up to one year full time on exploratory development and problem-solving efforts with the post-doctorals splitting their time between the customer location and their educational institutions. The program is totally customer-funded with current projects being undertaken for Rome Air Development Center (RADC), Space and Missile

Systems Organization (SAMSO), Aeronautical Systems Division (ASD), Electronic Systems Division (ESD), Air Force Avionics Laboratory (AFAL), Foreign Technology Division (FTD), Air Force Weapons Laboratory (AFWL), Armament Development and Test Center (ADTC), Air Force Communications Service (AFCS), Aerospace Devense Command (ADC), Hq USAF, Defense Communications Agency (DCA), Navy, Army, Aerospace Medical Division (AMD), and Federal Aviation Administration (FAA).

Further information about the RADC Post-Doctoral Program can be obtained from Jacob Scherer, RADC/RBC, Griffiss AFB, NY, 13441, telephone AV 587-2543, COMM (315) 330-2543.

CONTENTS

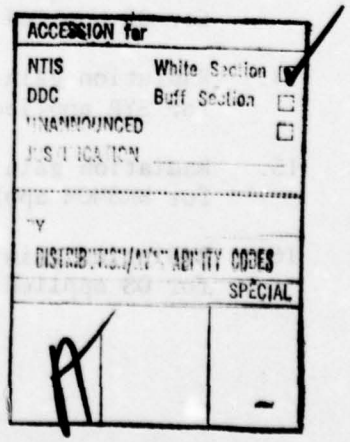

LIST OF FIGURES

LIST OF TABLES

1. INTRODUCTION

Recently developed numerical methods have been applied successfully to performance prediction of antennas in complex scattering environments. The general framework for these techniques, at frequencies for which the antenna* is at most a few wavelengths, is the method of moments (moment method) as set forth by Harrington [Harrington 1968]. Many computer programs have been developed, based on the moment method. A number of them are applicable to solving antenna problems of quite arbitrary geometries. In particular the programs based upon thin-wire modeling are applicable. Not all antennas are collections of thin wires, however. Hence, there are two concerns regarding these methods: (a) the accuracy of the model, and (b) the accuracy of the analysis of the model. An accurate model is one which exhibits all important aspects of the actual antenna. This accuracy can be gauged either by (1) comparison with experiment or other analysis if results from these exist, or (2) continuously increasing the complexity of the model (add wires, for example) until computed parameters such as driving point impedance, radiation pattern, or current show little change. Gauge (2) is a convergence test.

An accurate model analysis, on the other hand, is not related to the relevance of the model, but rather to the accuracy with which an analytical tool predicts important model parameters. For example, a thin-wire moment

*The word "antenna" as used throughout this report is intended to mean "antenna and its environment".

method computer program could be applied to a wire-gridded model of a corner reflector antenna to determine its radiation pattern. The result might accurately predict the model's pattern. However, this pattern may differ significantly from that of the actual corner reflector.

This report is concerned only with the accuracies of moment methods given a thin-wire model. In particular, three currently available and often used computer programs are compared by their application to simple and complex antenna models. Of interest are not highly accurate predictions of current. Instead, "reasonable" values (within $\sim$ 3 dB of converged values) of driving point impedance and radiation patterns (far-field) are sought. The principal variable is expansion function number N, and a program which generally gives satisfactory results for least N is considered superior.

A number of thin-wire moment method computer program comparisons have been conducted previously [Miller 1974, Butler 1975, Baldwin 1974, Logan 1973, Rogers 1974]. However, these comparisons either (a) considered only scattering, (b) sought high accuracy in current which requires many expansion functions per wavelength λ, (c) considered relatively simple shapes such as the straight wire, "L" shaped wire (2-wire junction), or crossed wires (4-wire junction), or (d) a combination of the above.

In many applications, such as shipboard antenna performance prediction, the complexity of the problem often precludes high accuracy. However, less accurate predictions are often satisfactory. Also, the principal parameters are usually radiation patterns and driving point impedance -- not current. Therefore, the computer program comparisons presented here should be of interest to many designers or analyzers of antenna environments. With

regard to shipboard applications, a general assessment of moment methods is available [Buchanan et al. 1977].

In Sections 2 and 3 a review of thin-wire moment method modeling is presented. In Section 4 three computer programs, differing primarily in choice of expansion and testing functions, are discussed. The means for comparing these programs is detailed in Section 5. Finally, in Section 6 the programs are compared by presenting driving point impedance and radiation pattern computations. These results are obtained by considering four different wire models -- two simple and two complex -- each with increasing numbers of expansion functions. Computer run time is also considered.

2. THIN WIRE ANTENNA THEORY

The most popular formulations for solving thin-wire antenna problems are of the $\underset{\sim}{E}$-field type. The wire surface current $\underset{\sim}{J}$ is sought such that the $\underset{\sim}{E}$-field it radiates satisfies the condition

$$\underset{\sim}{E}\big|_{tan} = \begin{cases} 0 \text{ on perfect conducting surface of wire} \\ \text{applied field at location of excitation (gap) on wire} \end{cases} \tag{1}$$

where $|_{tan}$ signifies "component tangential to wire surface." Two simplifications are usually invoked prior to implementing these formulations. First, the thin-wire approximation is made. With reference to Figure 1 this approximation assumes (a) there is no circumferentially directed component of $\underset{\sim}{J}$, (b) $\underset{\sim}{J}$ is replaced by a filiament of current I located along the wire axis C', (c) equation (1) is satisfied along a line C parallel to the wire axis and offset a wire radius a from the axis, and (d) equation (1) is

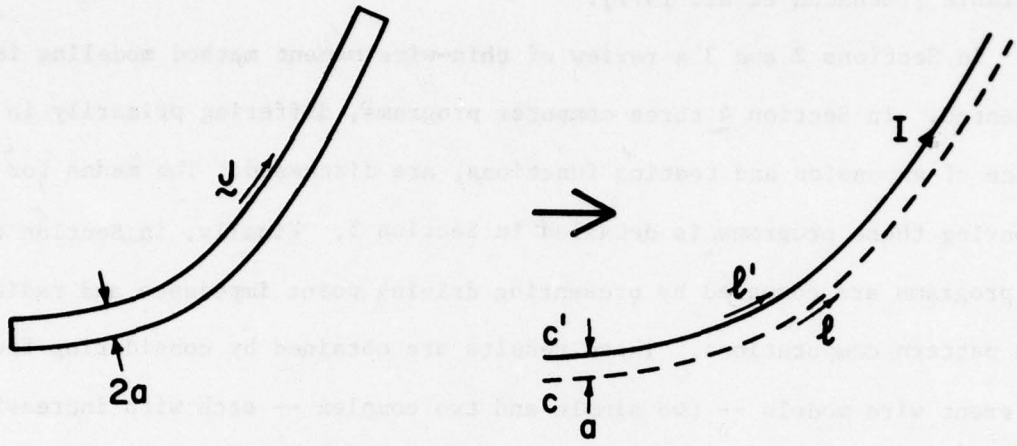

Figure 1. Arbitrary wire and thin wire approximation.

Figure 2. Choice of positive reference for voltage excitation.

applied only to the axial component of $\underset{\sim}{E}$. Points along C' are defined by the length variable ℓ' and those along C by ℓ.

The second simplification often used is that the ith applied field is specified as a finite voltage $\hat{V}_i$ over a small gap (delta gap excitation). Thus (1) becomes

$$L(I,\ell) = \sum_i \hat{V}_i \delta(\ell - \ell_i) \tag{2}$$

where

$$L(I,\ell) = -\underset{\sim}{E}\cdot\hat{\ell} \tag{3}$$

the ℓ_i are the locations of applied voltage excitations $\hat{V}_i$ referenced as shown in Figure 2 and $\hat{\ell}$ denotes a unit vector at ℓ oriented parallel to C.

Most frequency domain, moment method, thin-wire computer programs are based on one of two forms for the operator L.

A. Potential Integrodifferential Equation

Here L has the form [Harrington 1968 (Chapter 4)]

$$L(I,\ell) = j\omega\mu\int_{C'} \hat{\ell}\cdot\hat{\ell}' I(\ell')G(\ell,\ell')d\ell' - \frac{1}{j\omega\varepsilon}\frac{d}{d\ell}\int_{C'} \frac{dI(\ell')}{d\ell'} G(\ell,\ell')d\ell' \tag{4}$$

where

$$G(\ell,\ell') = \frac{e^{-jkR}}{4\pi R} \tag{5}$$

and R is the distance between a "source" point at ℓ' ($\hat{\ell}'$ is corresponding unit vector) on the wire axis C' and a "field" point at ℓ on the wire surface path C. The remaining variables have their usual meanings.

B. Pocklington's Equation

Here L has the form [Miller 1974]

$$L(I,\ell) = \frac{1}{j\omega\varepsilon} \int_{C'} I(\ell')\left(\frac{\partial}{\partial \ell}\frac{\partial}{\partial \ell'} - k^2 \hat{\ell}\cdot\hat{\ell}'\right)G(\ell,\ell')d\ell' \qquad (6)$$

where $k^2 = \omega^2\mu\varepsilon$.

A major difference between these two formulations is that (4) involves derivatives of the unknown current I and (6) involves derivatives of the Green's function G. For a finite wire radius (4) and (6) can be derived from one another. Thus exact solutions, if they exist, are independent of the formulation used to obtain them. However, when approximate solutions are sought, as via the moment method, the particular formulation used may have a significant effect on convergence, computational ease, etc.

A third form for L results from an extension of Hallen's integral equation [Butler 1972]. Hallen's equation is devoid of derivatives, thus eliminating associated computational difficulties. This form, however, is complicated by the introduction of unknown constants that need solving along with the current. Also Butler's form, although permitting wire juntions, is restricted to straight wire configurations. Other modifications of Hallen's form applicable to curved wires [Mei 1965] and curved wires with junctions [Taylor 1969] suffer from additional operator complexities. For perhaps these reasons the authors are not aware of a user-oriented, arbitrary-wire-geometry computer program based on a Hallen's type integral equation. This is not a severe omission, however, for the following reason. Equation (2) must be approximated by a linear system of equations before it can be solved for arbitrary geometries. This approximation, the crux of the moment method which will be discussed shortly, involves integrating both sides of (2) after

multiplication by a testing (or weighting) function. There is a wide class of testing functions to choose from, and it is shown by Wilton and Butler [Wilton 1976] that a particular weighting of Pocklington's Equation is equivalent to another weighting of Hallen's Equation.

3. METHOD OF MOMENTS

The method of moments (or moment method) is a unifying concept for reducing a linear, inhomogeneous integrodifferential equation such as (2) to a set of simultaneous, linear, algebraic equations. In matrix form the latter becomes

$$[Z]\bar{I} = \bar{V} \tag{7}$$

where $[Z]$ is a known square matrix and $\bar{V}$ and $\bar{I}$ are known and unknown column vectors respectively. An in-depth treatment of the moment method is given by Harrington [Harrington, 1968]. Once suitable $[Z]$ and $\bar{V}$ are known (7) can be solved for $\bar{I}$. The elements of $\bar{I}$ are the coefficients in an expansion of the solution to the original equation. Only $\bar{V}$ contains information on the sources of the original equation. Thus $[Z]$ need be computed only once to solve a time-harmonic problem of a particular geometry and frequency but where the source distribution varies.

Equation (7) is of a form often appearing in network theory as relating voltages and currents of an N-port network. Thus $[Z]$ is often referred to as the "generalized impedance" matrix and $\bar{I}$ and $\bar{V}$ the "generalized current" and "generalized voltage" vectors respectively.

The process of reducing (2) to (7) begins with the selection of a set of N independent functions $\{f_n\}$ defined on C' with which to expand I. Thus

$$I(\ell') = \sum_{n=1}^{N} I_n f_n(\ell') \tag{8}$$

where the coefficients I_n are unknown. A set of N independent testing functions $\{g_m\}$ defined on C are then chosen. Finally a suitable inner product [Harrington 1968] usually of the form

$$\langle \phi_1, \phi_2 \rangle = \int_C \phi_1(\ell)\phi_2(\ell)d\ell \tag{9}$$

is chosen and the inner product of each side of (2) is taken after multiplication of both sides with each g_m. The resulting N equations in N unknowns (the I_n) are expressed in matrix form by (7) where the nth element of $\bar{I}$ is I_n, the mth element of $\bar{V}$ is

$$V_m = \sum_i \hat{V}_i g_m(\ell_i) \tag{10}$$

and the m,nth element of [Z] is

$$Z_{mn} = \int_C g_m(\ell)L(f_n,\ell)d\ell \tag{11}$$

3.1 Basis Functions

The "expansion" or "basis" functions f_n, with which I is expanded, must be independent. Also the f_n should be chosen to well approximate a basis for the domain of L. One expects that f_n individually exhibiting characteristics of I will result in fewer of them and consequently less effort to solve (7). Thus the f_n are usually chosen to force I to satisfy current continuity at each point along C'. This implies that the f_n should be continuous along a wire excluding a junction point formed by

three or more wires and that $f_n = 0$ at a wire end. Also at a multi-wire junction the f_n from each of the wires are often distributed such that the total junction current satisfies continuity.

Occasionally the f_n are not within the domain of L. For example pulse functions (constant over a small region of C' and zero elsewhere) are not within the domain of L as given by (4). However, such simple basis functions can still be used if L is "approximated", for example, with a finite-difference evaluation of the derivatives. The computer program WRSMOM, which is discussed later, is based on pulse expansion functions with a finite-difference approximation to L. Further discussions concerning "approximate operators" and other techniques such as "extended domains", etc. are given in [Harrington 1968].

The f_n are generally composed of one of two function types -- entire functions or subsectional functions. Subsectional functions are each defined other than zero only over a small region of C'. An example is the pulse functions discussed above. Entire functions are not so constrained. Examples of entire function bases are Maclaurin Series polynomials, Fourier trigonometric functions and Legendre polynomials. These three bases are comprised of independent functions. In addition, the latter two are comprised of functions orthogonal with respect to (9). However, neither basis necessarily orthogonalizes L ($\langle \phi_1, L\phi_2 \rangle = 0$ if $\phi_1 \neq \phi_2$) which would result in diagonal [Z]. A set of functions which does diagonalize [Z] would, of course, form an excellent basis but, for arbitrary geometries such a set of functions is costly to compute. (The class of rotationally symmetric bodies is an exception in that basis functions with sinusoidal circumferential variation are

known to "block" orthogonalize L [Harrington 1969, Mautz 1977].)

Experience indicates that entire function expansions tend to converge faster than subsectional function expansions [Thiele 1973]. However, the latter tends to result in "better conditioned" [Z] matrices in that the ratio of diagonal to off-diagonal [Z] elements has generally greater magnitude. A procedure for solving (7) when [Z] is better conditioned is generally less sensitive to round-off errors.

The computation of [Z] for an entire function expansion is usually considerably more involved than for a subsectional function expansion. Thus for complex wire geometry problems a subsectional function expansion is more inviting than an entire function expansion. Hence, the vast majority of available moment method computer programs for modeling arbitrary collections of bent wires are based on subsectional function expansions. Three examples of subsectional functions are shown in Figure 3. The f_n in 3(a) are pulses defined by

$$f_n(\ell') = \begin{cases} 1 & \ell_n - \Delta_n/2 < \ell' < \ell_n + \Delta_n/2 \\ 0 & \text{Otherwise} \end{cases} \tag{12}$$

where Δ_n is the pulse width defined in the figure. The f_n in 3(b) are overlapping triangles given by

$$f_n(\ell') = \begin{cases} (\ell' - \ell_{n-1})/\Delta_n^- & \ell_{n-1} \leq \ell' \leq \ell_n \\ (\ell_{n+1} - \ell')/\Delta_n^+ & \ell_n \leq \ell' \leq \ell_{n+1} \\ 0 & \text{Otherwise} \end{cases} \tag{13}$$

where Δ_n^- and Δ_n^+ are defined in the figure. The f_n in 3(c) are overlapping sinusoids given by

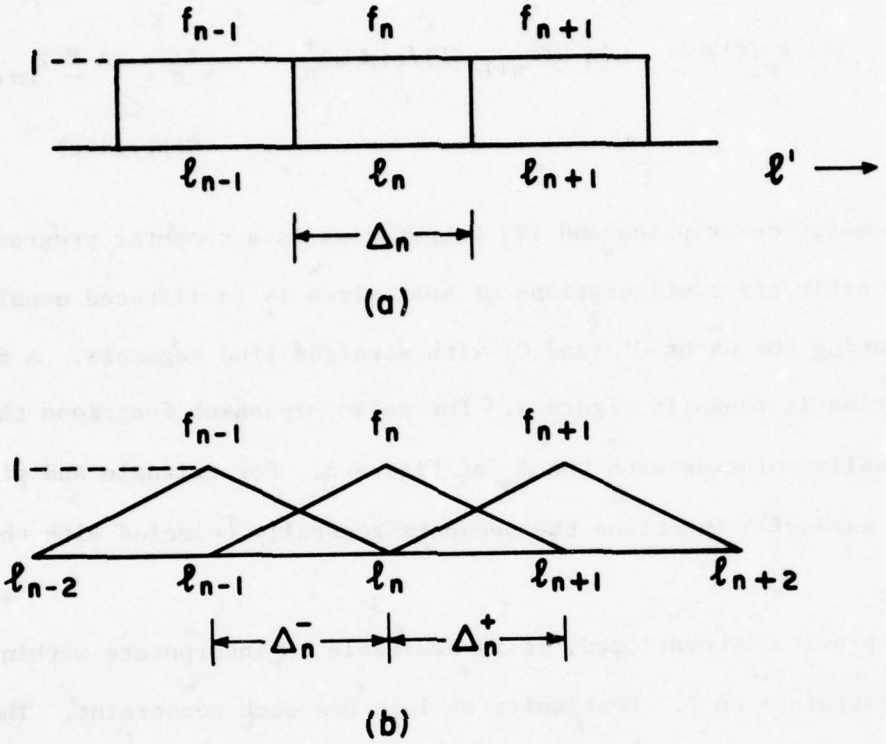

Figure 3. Subsectional functions: (a) pulse (piece-wise constant), (b) triangular (piece-wise linear), and (c) piece-wise sinusoidal.

$$f_n(\ell') = \begin{cases} \sin k(\ell'-\ell_{n-1})/\sin k\Delta_n^- & \ell_{n-1} \leq \ell' \leq \ell_n \\ \sin k(\ell_{n+1}-\ell')/\sin k\Delta_n^+ & \ell_n \leq \ell' \leq \ell_{n+1} \\ 0 & \text{Otherwise} \end{cases} \tag{14}$$

Geometry description and [Z] computation in a computer program applicable to arbitrary configurations of bent wires is facilitated usually by approximating the paths C' (and C) with straight line segments. A typical segmentation is shown in Figure 4. For pulse expansion functions the segments usually coincide with the Δ_n of Figure 3. For triangle and piece-wise sinusoid expansion functions the segments generally coincide with the Δ_n^- (and Δ_n^+).

As previously mentioned, it is desirable to incorporate within the f_n known constraints on I. Continuity of I is one such constraint. The pulse functions of Figure 3(a) do not enforce continuity of I. However, they are generally used in conjunction with approximate operators that afford additional smoothing. The triangle and sinusoid (piece-wise) functions of Figure 3(b,c), on the other hand, do enforce continuity of current at each point along C'. These two bases also maintain continuity of current at mutliple-wire junctions if a simple rule is followed in modeling the wires. To illustrate, consider the 3-wire junction shown in Figure 5(a). The modeling begins by choosing <u>any</u> one of the wires as terminated at the junction (Figure 5(b)). Then the remaining wires are added in succession such that each overlaps <u>any</u> previously placed wire (Figure 5(c,d)). This overlapping is accomplished by aligning the junction point with the peak of the

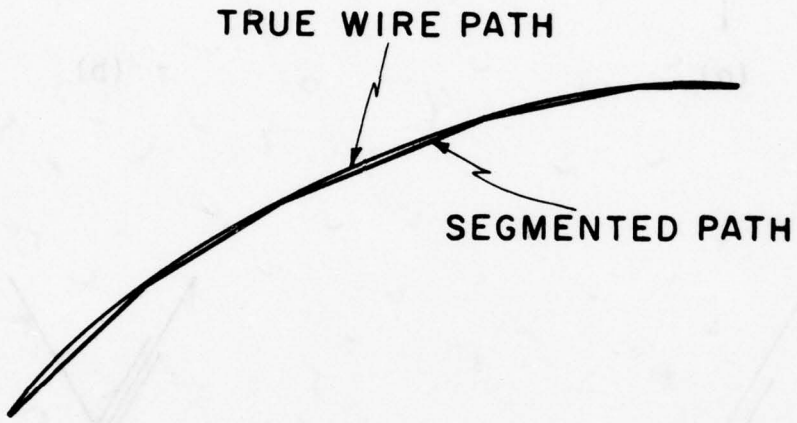

Figure 4. Segmentation of a wire.

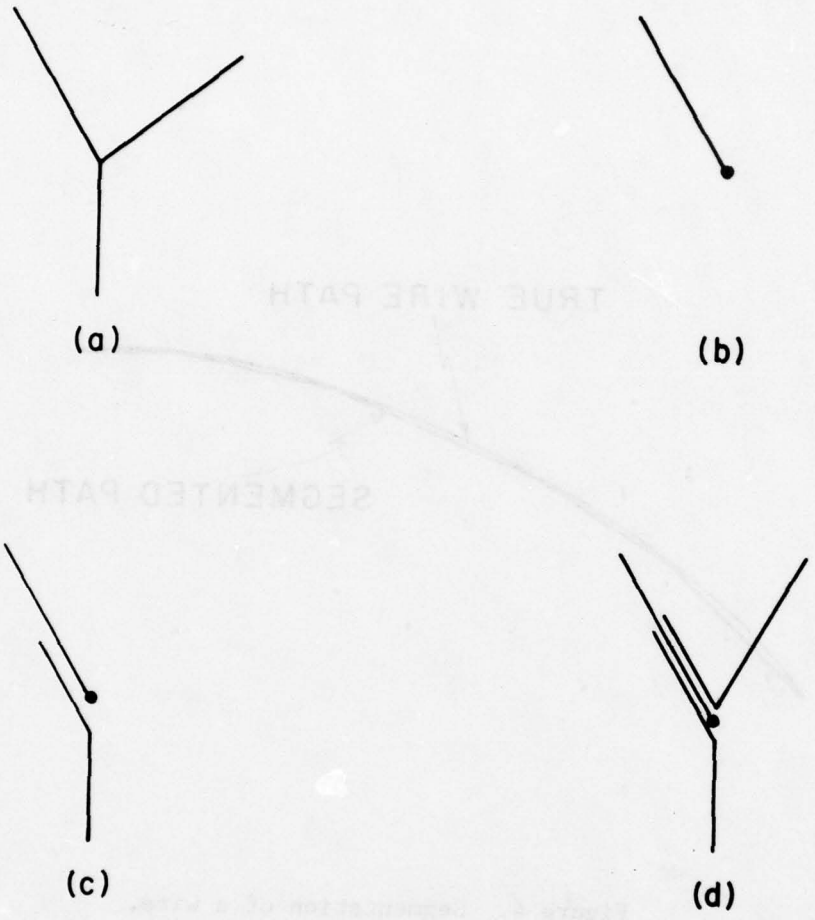

Figure 5. (a) A 3-wire junction. (b) One wire chosen terminated at junction. (c) Addition of a second wire by overlapping first wire. (d) Addition of a third wire also by overlapping first wire.

end triangle (or sinusoid) function on the wire being added. The justification for this method is given in [Chao 1970]. It is also presented in terms of "independent loop currents" in [Richmond (no date)].

3.2 Testing Functions

The set of testing functions $\{g_m\}$ must also be independent. Other restrictions on the g_m are not obvious from their explicit use as indicated by (10) and (11). However, one notes that the moment method is equivalent to the Rayleigh-Ritz procedure if the g_m are in the domain of L^a the adjoint operator of L [Harrington 1968] defined by

$$\langle \phi_1, L\phi_2 \rangle = \langle L^a \phi_2, \phi_1 \rangle$$

This equivalence is noteworthy since the Rayleigh-Ritz procedure achieves an approximate solution to a variational expression for a scalar quantity ρ of interest (impedance, far-field, etc.), i.e. small errors in I when used to compute a variational expression for ρ result in proportionately less error in ρ. For the "symmetric" inner product defined by (9) the operators of (4) and (6) are self-adjoint, i.e., $L^a = L$. Thus it is desirable to choose the g_m from the domain of L.

Two types of $\{g_m\}$ are often found in existing moment method computer programs. One type sets $\{g_m\} = \{f_n\}$. This is often called Galerkin's method. One advantage of Galerkin's method is that [Z] is then symmetric. This decreases the effort required for computing [Z] and for solving (7). It also saves computer storage since only the upper or lower triangle of [Z] is needed. A disadvantage is that the g_m may complicate the evaluation of (11). Examples of programs based on Galerkin's method are the Syracuse and

Ohio State programs (subsectional triangles and subsectional sinusoids respectively) discussed later.

The other frequently chosen $\{g_m\}$ is the set of impulses positioned at the centers of the f_n. This choice of g_m reduces the integral computation in (11) to a trivial operation. The choice of impulse functions for testing is also appropriately called "co-location" or "point-matching". Of course, these g_m are not within the domain of L. However, they are often used in conjunction with a finite-difference approximation to L which, as discussed earlier, provides a compensating smoothing effect. In fact, it has been shown that a finite-difference approximation to Pocklington's equation is closely akin to testing with triangles or sinusoids [Wilton 1976]. The computer program WRSMOM discussed later uses impulse testing.

Equation (10) takes a different form when g_m is an impulse function. *In this case the ith antenna excitation is generally treated as a specified* voltage $\hat{V}_i$ over a small but finite gap. The gap size is equal to the segment width Δ_{n_i} of the n_ith pulse expansion (basis) function occurring at the ith excited port. Then (2) becomes

$$L(I,\ell') = \sum_i \hat{V}_i \frac{1}{\Delta_{n_i}} \tag{15}$$

The testing functions are weighted impulses of the form

$$g_m = \delta(\ell - \ell_m)\Delta_m \tag{16}$$

Thus under impulse testing and pulse expansion (10) and (11) are replaced by

$$V_m = \begin{cases} \hat{V}_i & \text{if the ith excitation occurs at mth expansion function } (m=n_i) \\ 0 & \text{Otherwise} \end{cases} \tag{17}$$

$$Z_{mn} = L(f_n,\ell_m)\Delta_m \tag{18}$$

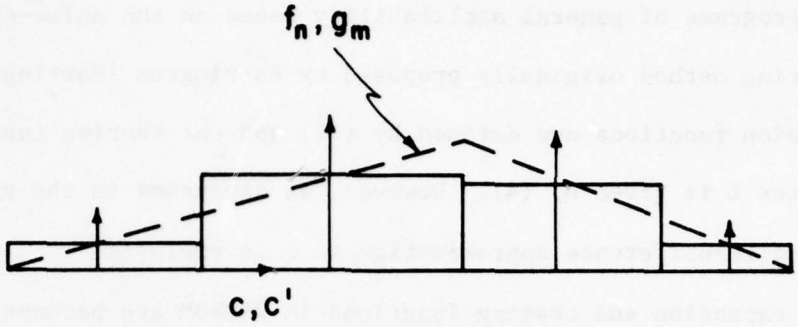

a) FOUR-PULSE APPROXIMATION TO $f_n(\ell')$ AND FOUR-IMPULSE APPROXIMATION TO $g_m(\ell)$

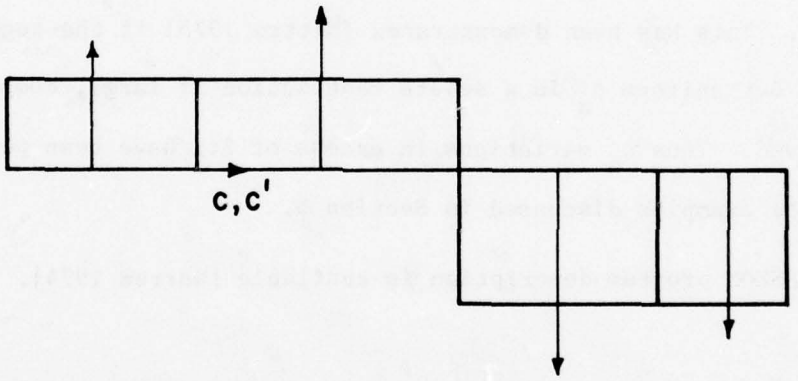

b) FOUR-PULSE APPROXIMATION TO $\frac{df_n(\ell')}{d\ell'}$ AND FOUR-IMPULSE APPROXIMATION TO $\frac{dg_m(\ell)}{d\ell}$

Figure 6. Syracuse program (SYR) treatment of (a) expansion and testing functions, and (b) their derivatives.

oriented programs of general applicability based on the pulse-expansion impulse-testing method originally proposed by Harrington [Harrington 1967]. The expansion functions are defined by (12) and the testing functions by (16). The operator L is given by (4). However, as discussed in the previous section, a finite-difference approximation to L is employed.

The expansion and testing functions in WRSMOM are perhaps the simplest feasible.* Thus [Z] is relatively simple to compute. However, [Z] is generally not symmetric.

The principal drawback to WRSMOM is that the pulse expansion functions do not constrain current continuity at not only multiwire junctions but also at segment-to-segment interfaces along a single wire. However, as previously mentioned, use of the approximate form of L tends to "smooth" these discontinuities. This has been demonstrated [Mittra 1975] if the segment sizes are uniform. But uniform Δ_n is a severe restriction if large, complex structures are involved. Thus Δ_n variations in excess of 2:1 have been permitted in some of the examples discussed in Section 6.

A WRSMOM program description is available [Warren 1974].

5. PROGRAM COMPARISON CONSIDERATIONS

Current itself is usually not of ultimate interest in the prediction or analysis of antenna performance. Radiation pattern and driving point impedance are usually the desired parameters. Once the current has been found,

*Impulse expansion functions (Hertzian dipoles), of course, are even simpler but they have shown promise only in "hybrid" programs. These programs use impulse expansion functions only for computing [Z] elements corresponding to distant current elements [Stewart 1974 (Section 3C)].

however, e.g., by the moment method, patterns and impedances are easily obtained. The three programs described in the last section each compute patterns and impedances. Therefore, a meaningful comparison between these programs is best made by assessing their relative ease in predicting patterns and impedances to within a desired accuracy for a variety of structures.

The accuracy of a method for predicting the EM characteristics of a complicated structure is difficult to assess. This is because of the scarcity of either exact solutions or reliable experimental results for complicated structures. Therefore, "correct" solutions are defined here as those values that all program results converge to that are reasonable. Program results converge if the addition of expansion functions does not appreciably change results.

Once converged parameter values (patterns and impedances) are obtained, a program is evaluated by its application with fewer and fewer expansion functions. A minimum number of expansion functions is determined when significant ($\sim$ 3dB) deviations from the converged values result. The program exhibiting smallest minimum is considered superior for that structure type. Of course, consideration must also be given to other variables contributing to computer run time and storage requirements. For example if OS requires more expansion functions than WRSMOM, it does not necessarily mean that the run time for computing [Z] ("matrix fill" time) is less for WRSMOM than for OS. Nor does it mean that the run time for solving (7) or even that the [Z] storage requirements are less for WRSMOM than for OS. This is because the symmetric matrix characteristic of OS gives it a significant advantage at the outset. Thus, although expansion function number is the principal

variable for program comparisons of the following section, the overall evaluation considers actual timing and storage.

Driving point impedance computations are considered within desired accuracy if both real and imaginary parts differ from converged values by at most a factor of ~ 2 (or $\sim 1/2$).

Radiation gain patterns are considered acceptable if they differ from converged patterns by at most $\sim$ 3dB at all pattern points.

In all cases the driving point impedance Z_{in} is computed as the ratio of the applied voltage $\hat{V}_1$ to the resulting coefficient I_{n_1} of current basis function at the location of the source. The radiation gain patterns are obtained by dividing 4π times the far-field intensity (for a desired polarization, θ or ϕ, of $\underset{\sim}{E}$-field) by the average input power P. Here P is determined from

$$P = |\hat{V}_1|^2 \text{ Real}\{1/Z_{in}\}$$

Note that $\hat{V}_1$ is an RMS value.

6. PROGRAM COMPARISONS

Results of applying the three computer programs OS, SYR, and WRSMOM to four thin-wire structures are discussed here. The first two structures considered are relatively simple: straight, resonant wire and three-wire junction. The second two are complex: whip-excited twin fan and self-excited twin fan. These structures are defined below.

As mentioned in Section 1 program comparisons with application to simple structures such as a straight wire and single three- or four-wire junctions have previously been reported on. The emphasis, however, was usually on obtaining a high degree of accuracy in current. Here, on the other hand,

the goal is to compare the computational efforts needed to obtain reasonable far-field and impedance values.

The coordinate system referred to throughout this section is shown in Figure 7. Also the variable for "number of expansion functions" is denoted N.

Except where otherwise mentioned, OS was run with the 4-interval Simpson's rule integration discussed in Section 4. The exception pertains to the self-excited twin fan example.

All examples have uniform wire radii since OS is not otherwise applicable. Of course, this could be a serious program constraint. However, as previously mentioned in Section 4, the many simplifying assumptions usually required in reducing a complex real-world structure to a tractable wire model are likely to dwarf that of uniform wire radius.

The distribution of expansion functions throughout a wire model was maintained approximately uniform whenever practical. A noted exception is the self-excited twin fan example where the excited wires are many times smaller than any of the other wires. This extreme wire-length variation provided a severe test for the three programs and thus served a purpose of this report. However, such difficulties can often be avoided by proper modeling. An example of a better model for the self-excited twin fan is discussed later. The self-excited twin fan example also violates the usual thin-wire criterion that the length L of each wire be many times the wire radius a. The excited wires have $L/2a \simeq 6$.

The whip-excited twin fan model has junctions with acute angles between wires as small as $\sim 15°$. This also provides a severe test for the thin-wire

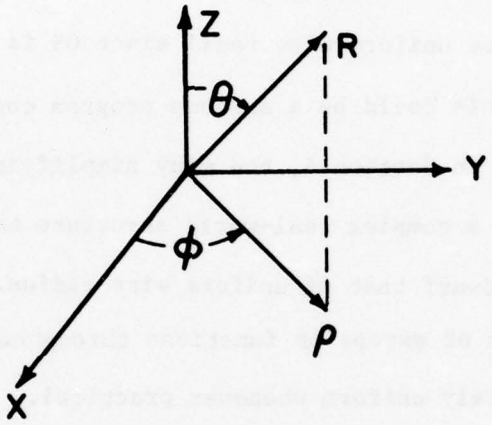

Figure 7. Coordinate system.

programs. Acute angles less than 30° are purported to be avoided [Richmond (no date)].

Many of the results were obtained with a minimum of expansion functions. Thus unusually large segment lengths Δ occurred. This necessitated bypassing a check incorporated in OS for "too-long" Δ's.

The Δ/a ratios were maintained significantly greater than unity. This is important since moment method solutions, with sinusoidal expansion functions, of problems modeled with and without the thin-wire approximation have been demonstrated to deviate significantly for $\Delta/a \simeq 1$ [Imbriale 1973]. In fact a diverging nature, not attributable to round-off error, of the solution with decreasing Δ/a was observed. In view of this and if it can be assumed that a subsectional basis is complete, then it follows that no solution exists for models incorporating the thin-wire approximation. Of course, approximate solutions such as those obtained with $\Delta/a > 1$ apparently do resemble the solution to actual wire problems. Thus solutions for thin-wire approximated models appear to asymptotically approach solutions for the actual wire models in that Δ/a must be neither too large nor too small.

6.1 Simple Structures

A. Resonant straight wire

This center-excited structure is shown in Figure 8. The frequency is 300 MHz. Table I gives the driving point impedances computed by the three programs for different numbers of expansion functions (N's). Equal length segments were maintained. For convenience, only odd N's were chosen since the wire is centrally excited. Reasonable agreement between the three

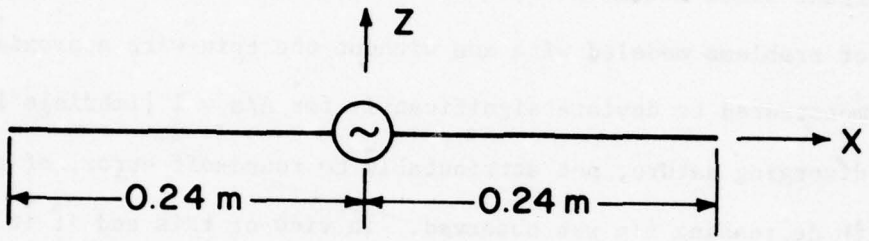

WIRE RADIUS = 10^{-4} m
EXCITATION = 1.0V
FREQUENCY = 300 MHz

Figure 8. Resonant straight wire.

TABLE I

Driving Point Impedance for Resonant Wire

No. of Expansion Functions (N)	Program OS	SYR	WRSMOM
21	70.3-j10.0	69.5-j13.8	69.5-j13.7
1	--	40.7-j145.6	46.8+j91.3
3	68.8-j12.2	59.3-j55.6	63.9+j5.0
5	69.5-j11.6	--	--
7	69.8-j11.2	66.7-j25.1	67.8-j12.5
11	70.0-j10.7	68.4-j18.4	68.7-j14.1

Dashed line underlines impedances which first fall within convergence criteria discussed in Section 5.

programs is apparent with N = 21 and the corresponding values were assumed correct. The dashed line underlines the impedances which first fall within convergence criteria discussed in Section 5. Thus OS demonstrates better convergence here. The OS program does not permit an N = 1 run. However, it is expected that the single expansion function case for OS would also give acceptable impedance values since it is simply the usual sinusoidal-current assumption [Jordan 1950 (pg 543)]. On the other hand, it is possible that SYR and WRSMOM runs with N = 5 would also be acceptable. These were not obtained at the time of data taking.

In Figures 9-11, X-Y plane radiation gain patterns are given for the ϕ component of $\underset{\sim}{E}$-field. The three programs display excellent results for the minimum number of expansion functions that can be applied.

B. Three-wire junction

This antenna is shown in Figure 12. The total wire length is $\sim 0.7\lambda$. Approximately equal segment lengths were maintained throughout. In Table II driving point impedances computed by the three programs again exhibit fastest convergence for OS. The minimum number of expansion functions N = 3 appears adequate for OS. This number is arrived at by centering one expansion function at the excitation and providing two more to satisfy current continuity at the junction as discussed in Sections 3 and 4.

In Figures 13-15 the X-Y plane radiation gain patterns for the θ component of $\underset{\sim}{E}$-field are given. All three programs provide acceptable (within 3 dB of converged pattern, as discussed in the previous section) results with the minimum number of expansion functions N = 3. However, the

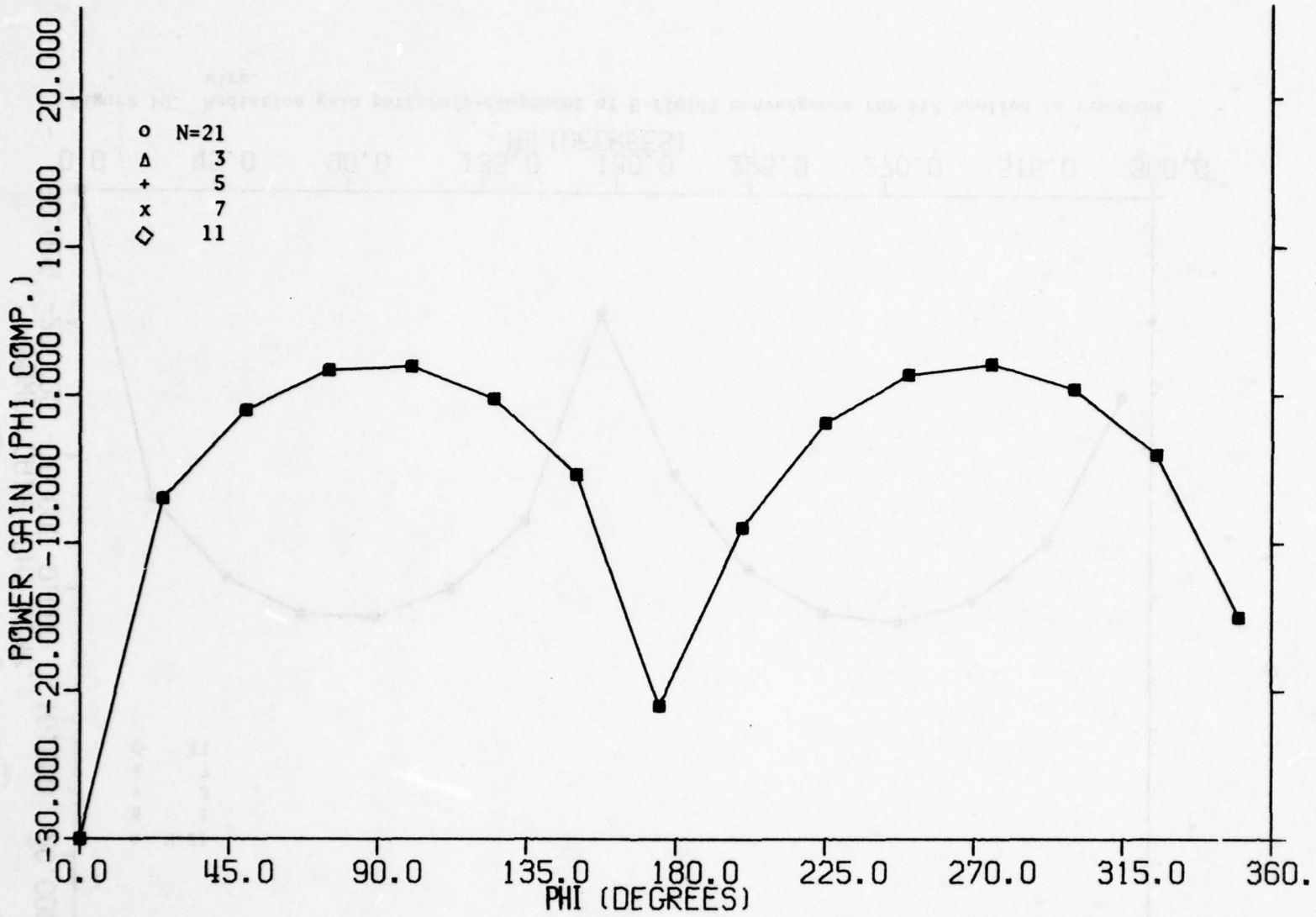

9. Radiation gain pattern (ϕ-component of $\underset{\sim}{E}$-field) convergence for OS applied to resonant wire.

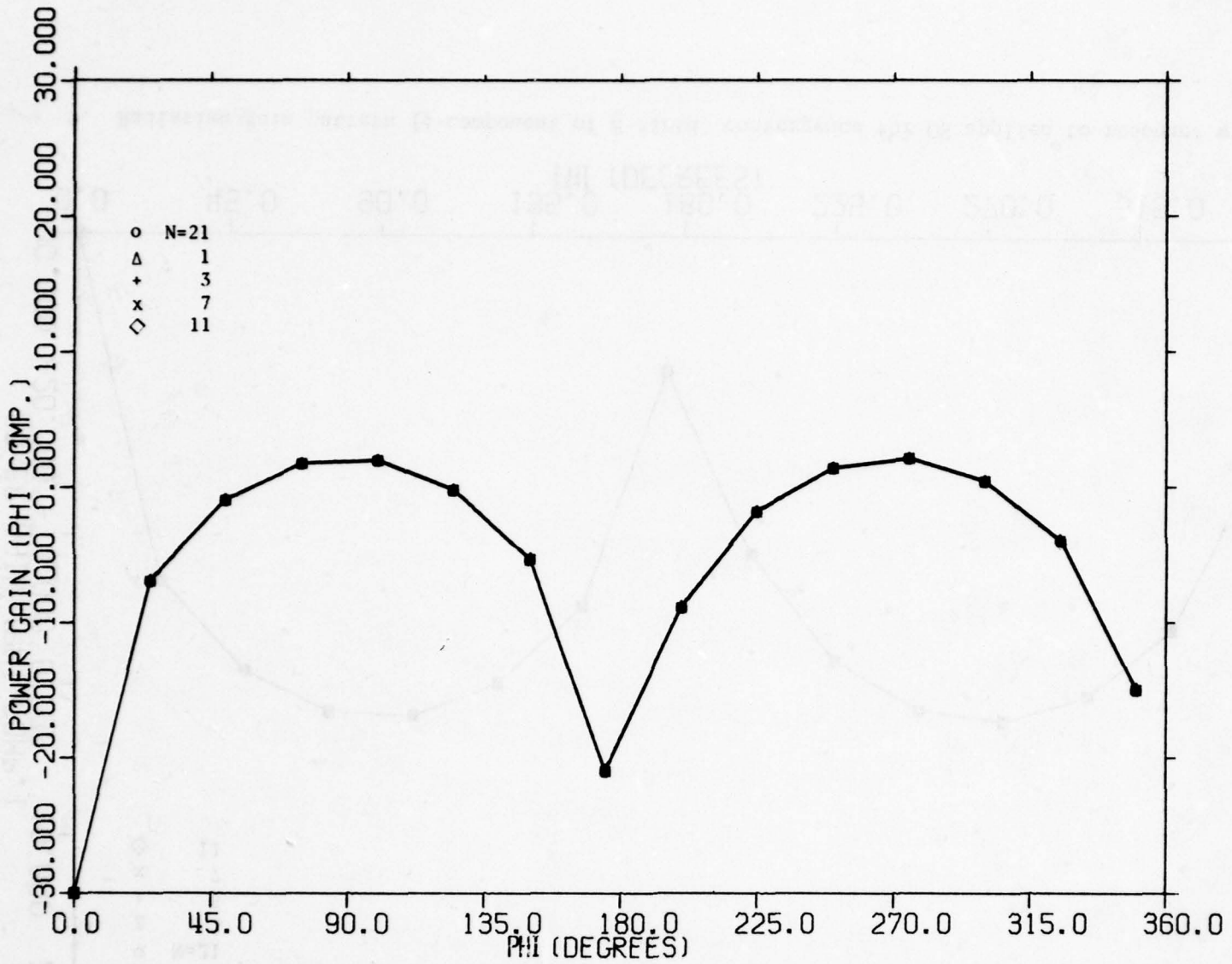

Figure 10. Radiation gain pattern(ϕ-component of $\underset{\sim}{E}$-field) convergence for SYR applied to resonant wire.

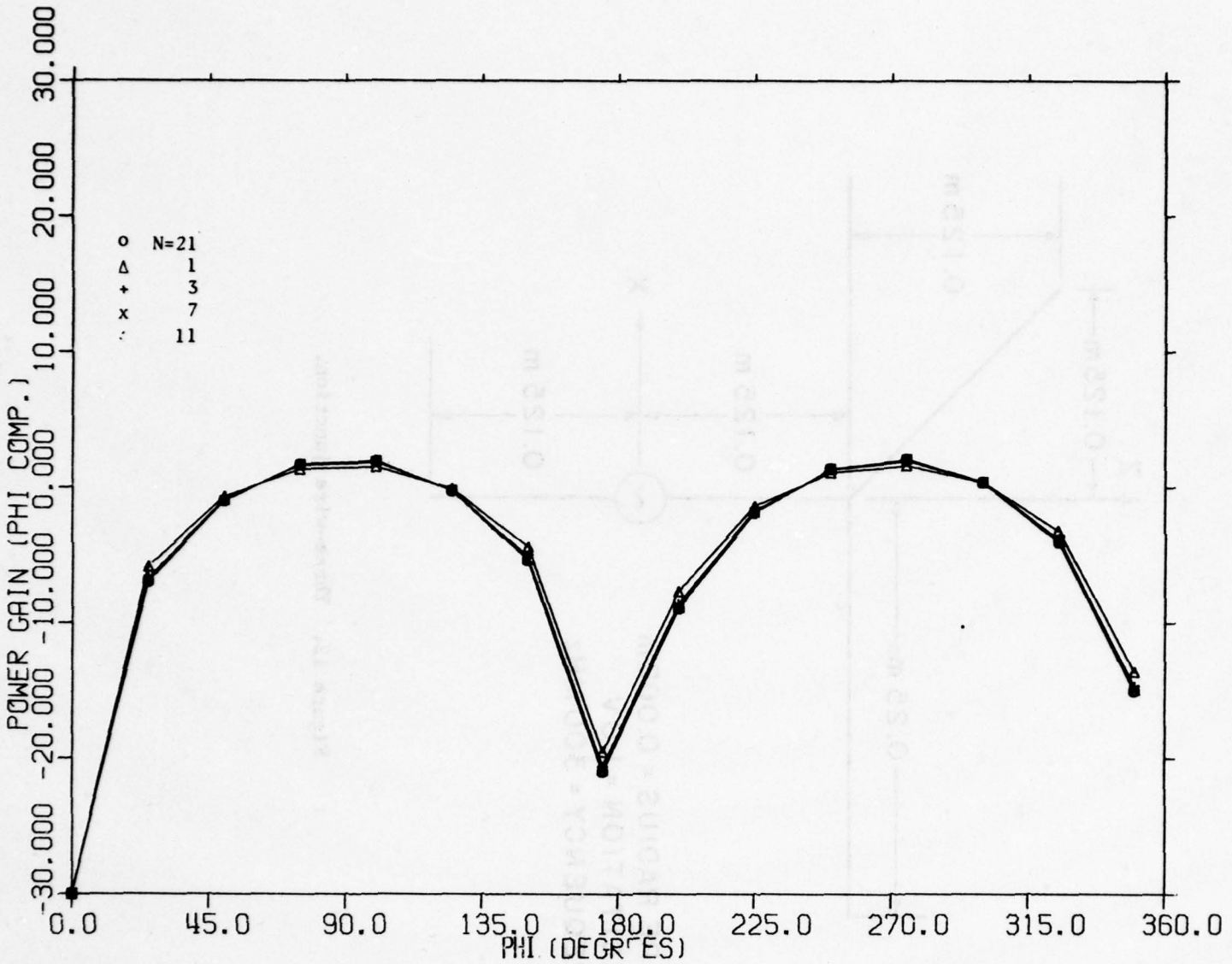

Figure 11. Radiation gain pattern (ϕ-component of $\underset{\sim}{E}$-field) convergence for WRSMOM applied to resonant wire.

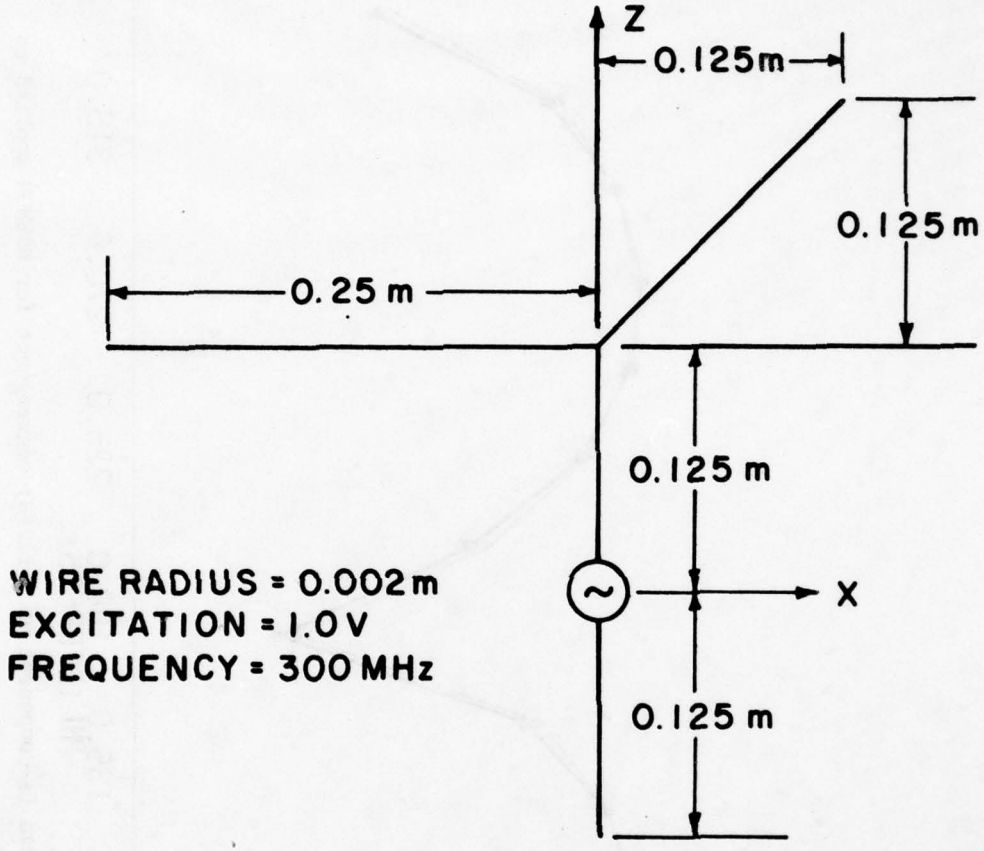

Figure 12. Three-wire junction.

TABLE II

Driving Point Impedance for Three Wire Junction

No. of Expansion Functions (N)	Program OS	SYR	WRSMOM
15*	82.1+j7.2	79.0+j3.0	75.0+j13.0
3	75.0+j3.7	46.3-j51.3	69.4+j47.4
6	78.7+j4.8	66.6-j11.2	87.7+j24.3
9**	80.9+j5.8	75.5-j2.0	71.4+j18.4
11***	81.2+j6.7	76.6+j1.3	89.3+j12.6

Dashed line underlines impedances which first fall within convergence criteria discussed in Section 5.

* 13 for WRSMOM

** 8 for WRSMOM

*** 10 for WRSMOM

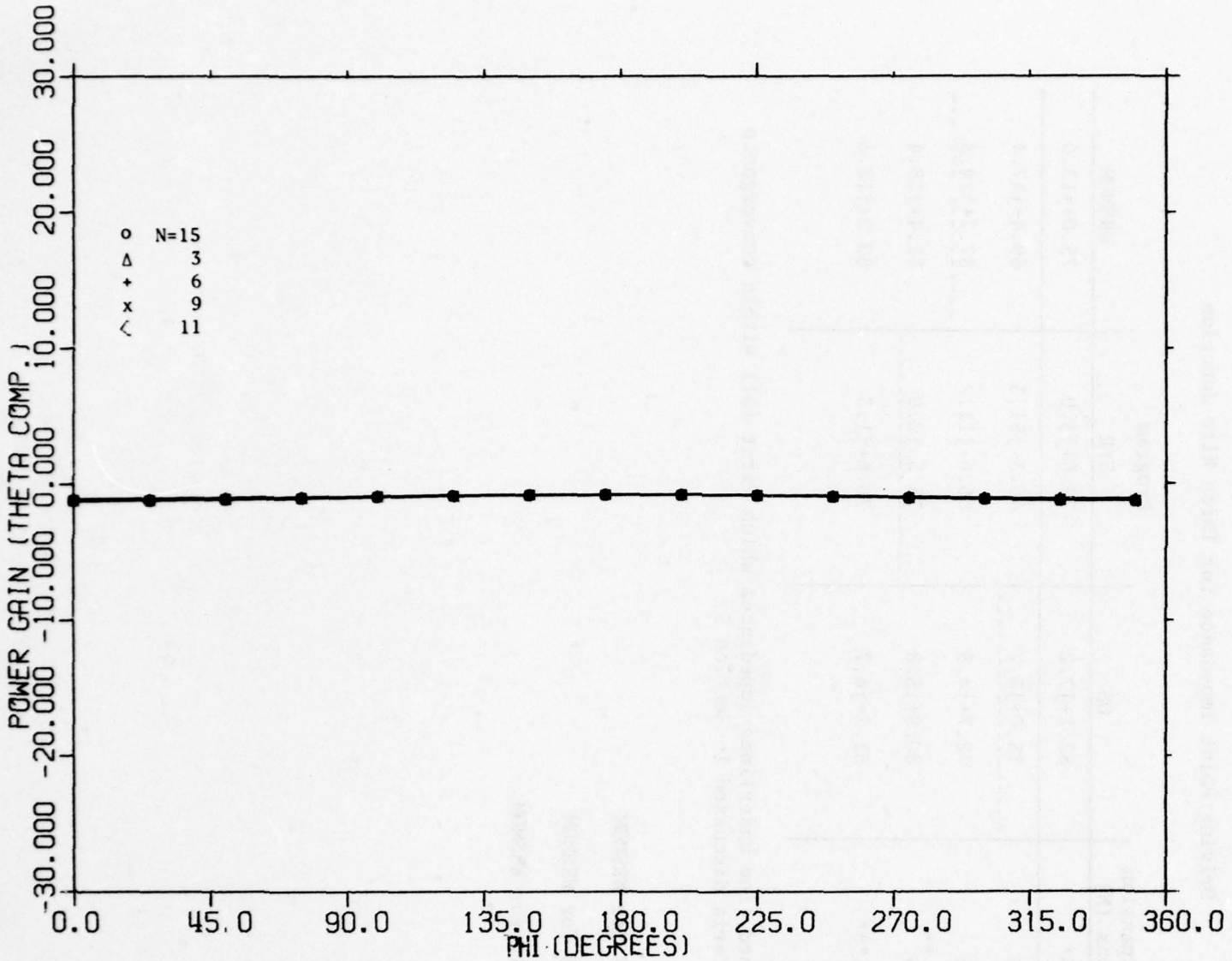

Figure 13. Radiation gain pattern (θ component of E-field) convergence for OS applied to three-wire junction antenna.

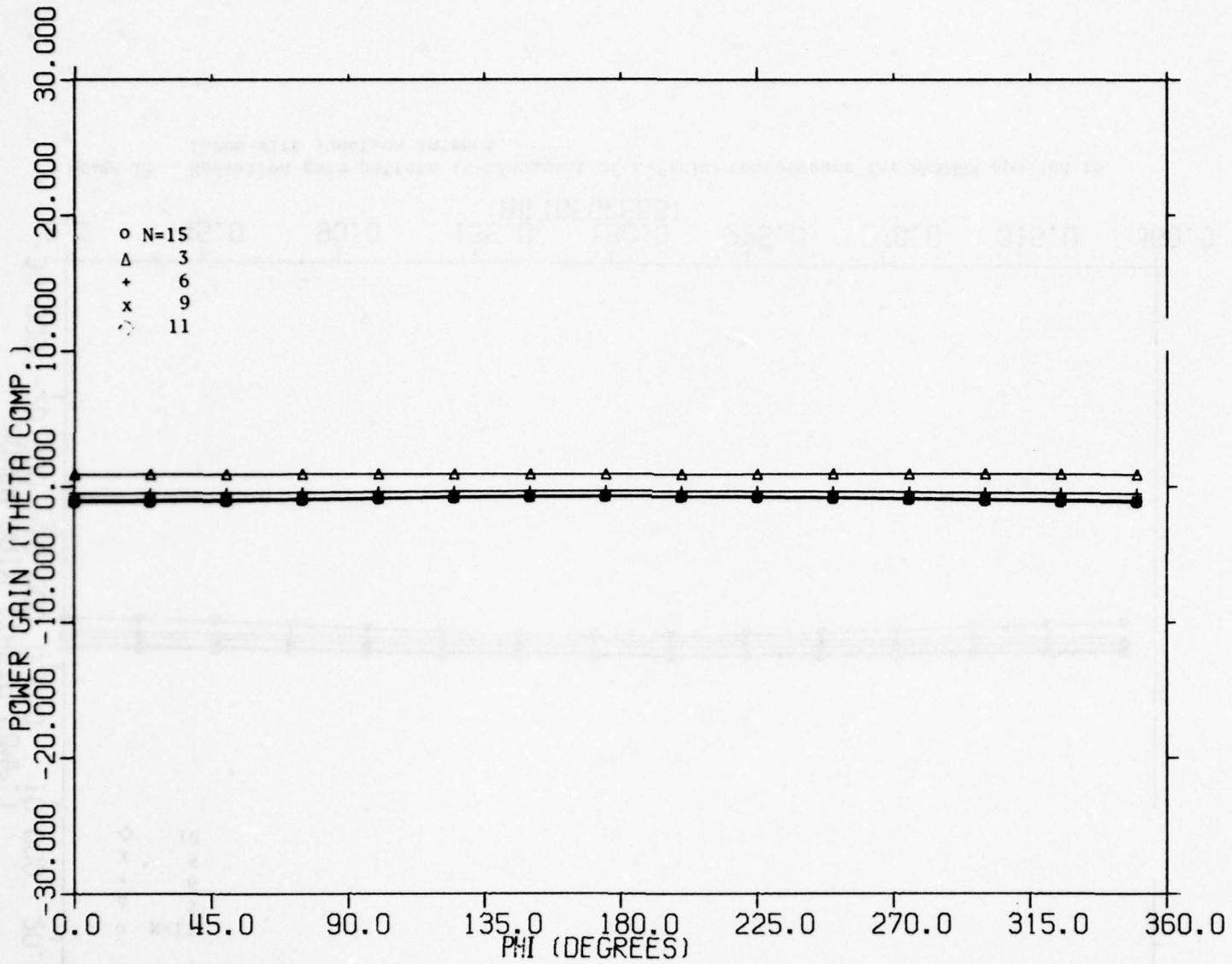

Figure 14. Radiation gain pattern (θ-component of E-field) convergence for SYR applied to three-wire junction antenna.

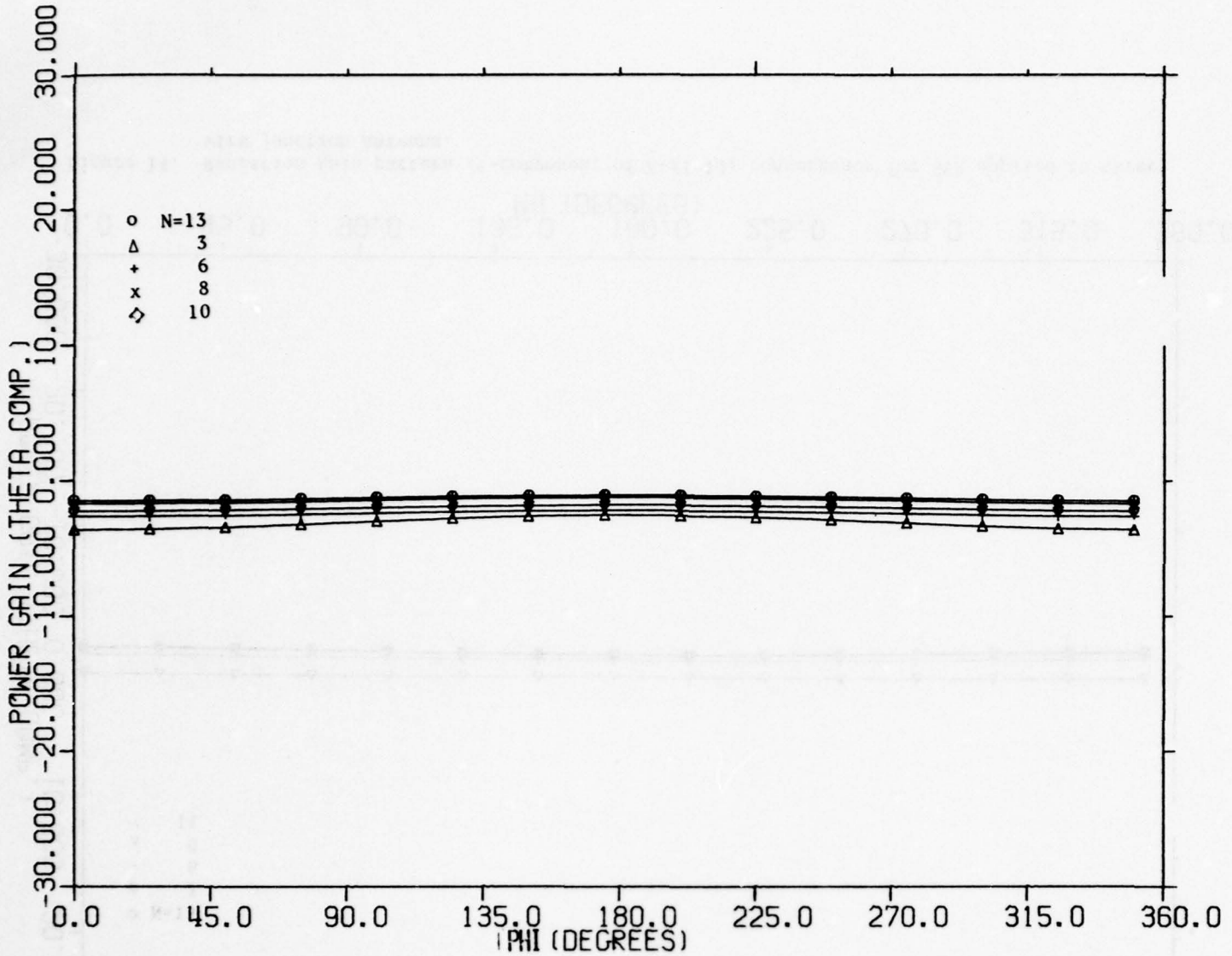

Figure 15. Radiation gain pattern (θ-component of E-field) convergence for WRSMOM applied to three-wire junction antenna.

convergence for OS (Figure 13) is exceptionally rapid.

In Figures 16-18 the ϕ component of $\underset{\sim}{E}$-field radiation gain patterns are plotted. Again the convergence for OS is exceptional (Figure 16), and the minimum N for WRSMOM is adequate (Figure 18). However, SYR appears to require additional expansion functions to achieve satisfactory results (Figure 17).

It is interesting that WRSMOM demonstrates at least as good convergence as SYR for this problem. Logan [Logan1973] also applied WRSMOM and SYR to a three-wire junction problem (albeit a configuration different from that of Figure 12). He found WRSMOM to be significantly less accurate than SYR which he attributed to the presence of the junction. However, a discussion with WRSMOM's author [Warren 1975] suggests that the presence of a large adjacent subsectional variation (> 2:1) is the real culprit in Logan's comparison. In Section 4 it was pointed out that the pulse expansion functions used in WRSMOM do not constrain current continuity even on single wires. Thus the junction presence alone should not cause large errors.

6.2 Complex Structures

A. Whip-excited twin fan

This structure is shown in Figure 19. The whip antenna is 5m from the simplified twin-fan model. A ground plane is assumed and thus the presence of the images. However, for generality the computer programs do not incorporate the simplifications made possible by this symmetry. The excitation port (at the 6-wire junction) of the twin-fan is assumed shorted.

A total of 18 wires comprises this model which includes two 6-wire

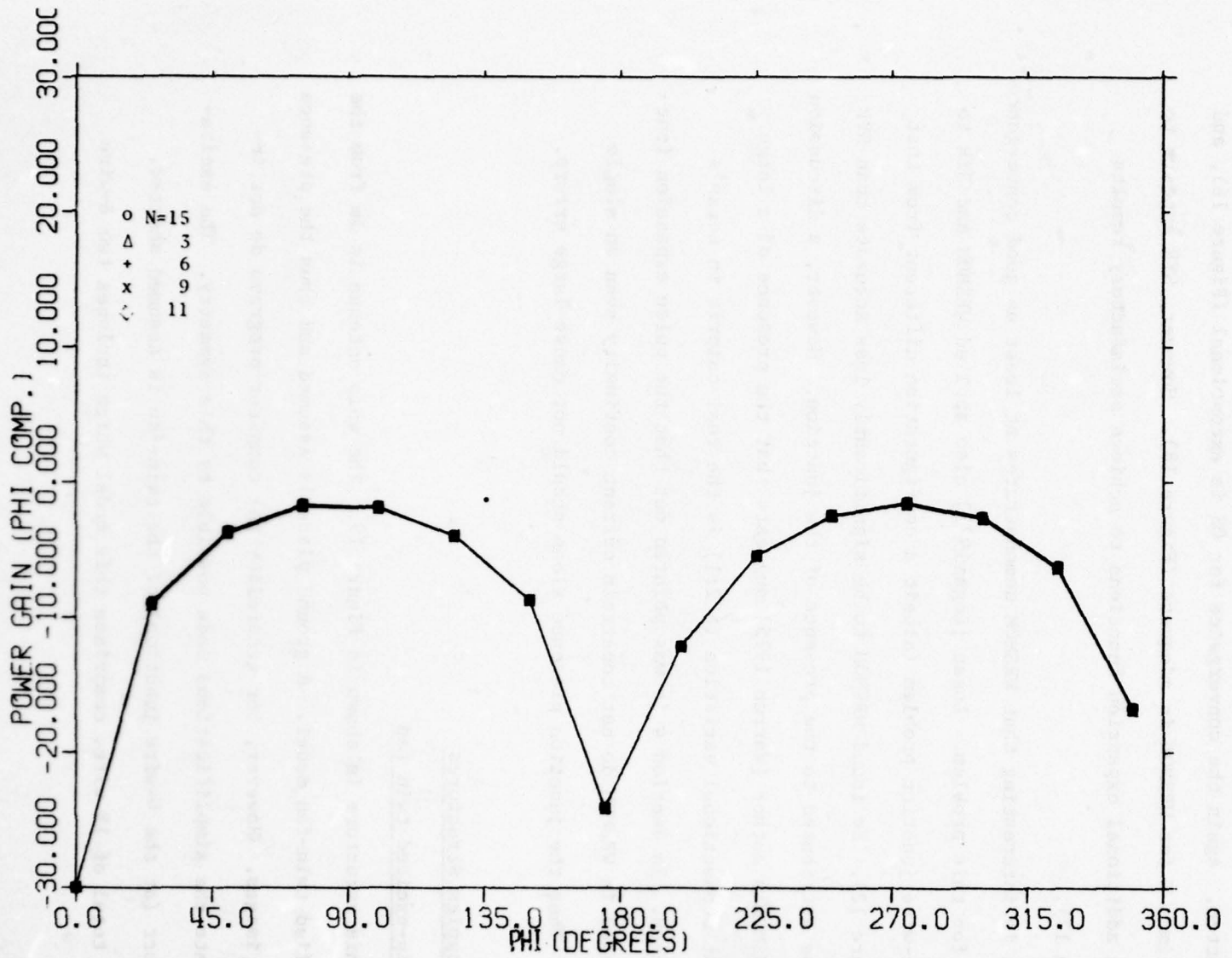

Figure 16. Radiation gain pattern (ϕ-component of $\underset{\sim}{E}$-field) convergence for OS applied to three-wire junction antenna.

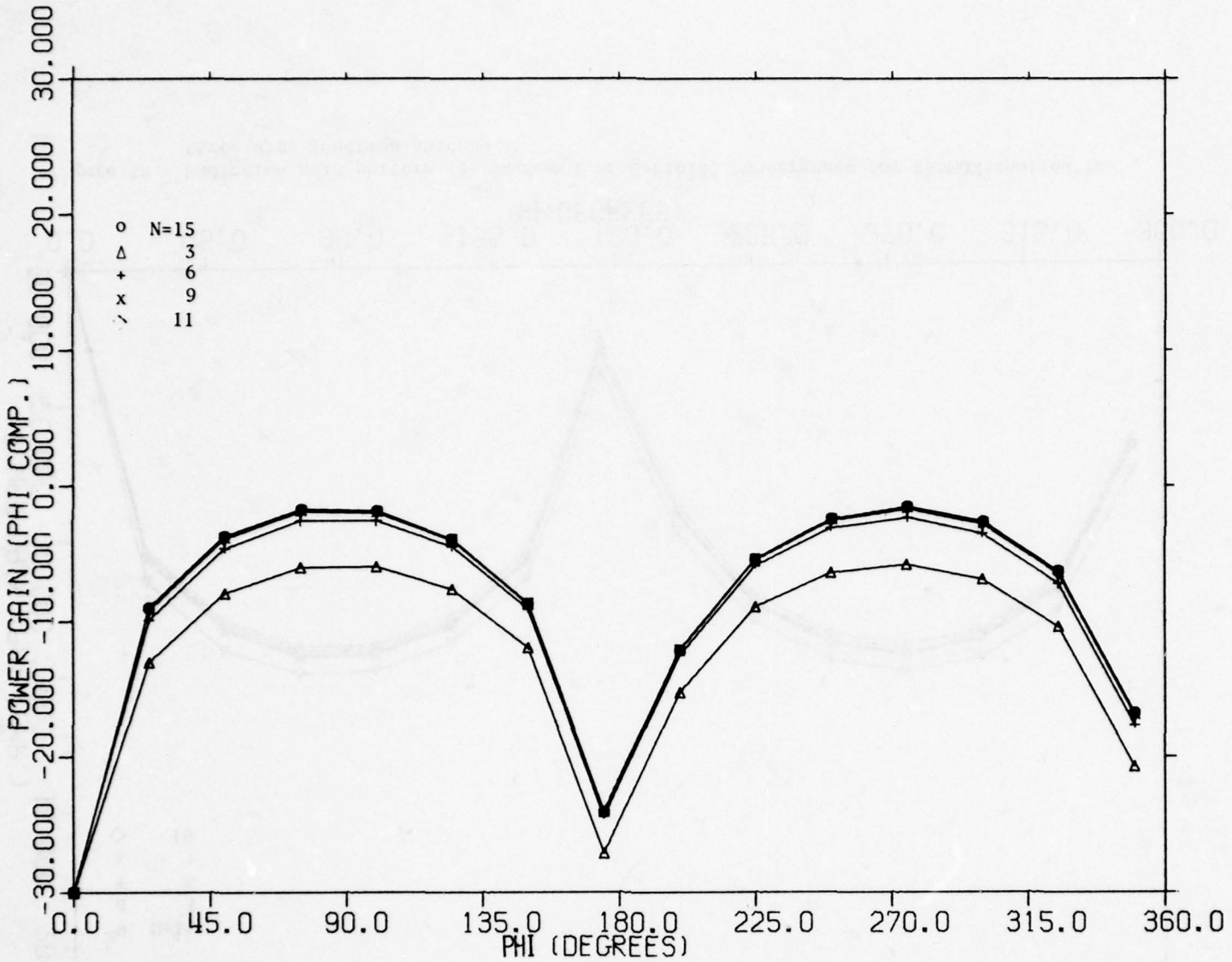

Figure 17. Radiation gain pattern (ϕ-component of $\underset{\sim}{E}$-field) convergence for SYR applied to three-wire junction antenna.

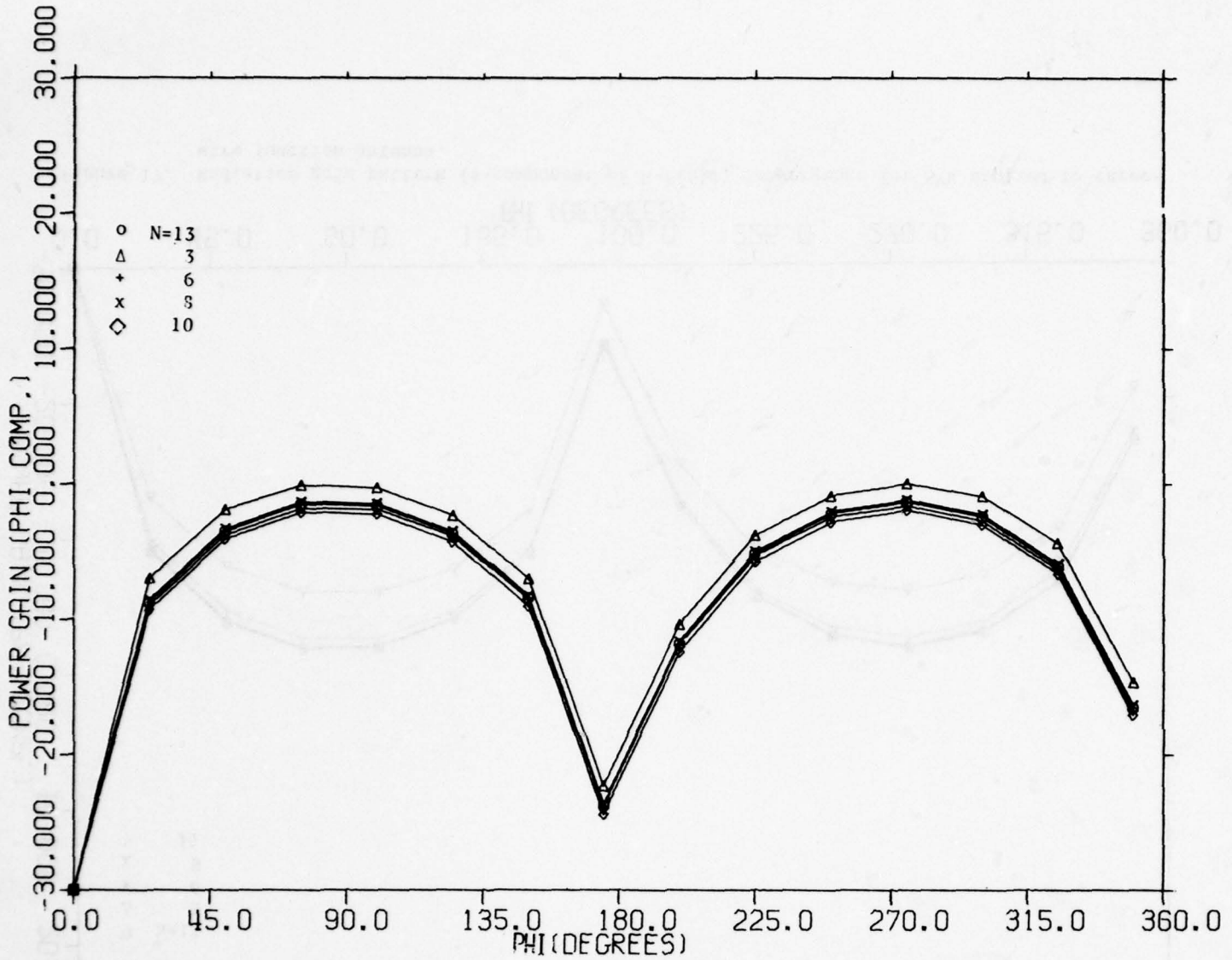

Figure 18. Radiation gain pattern (ϕ-component of $\underset{\sim}{E}$-field) convergence for WRSMOM applied to three-wire junction antenna.

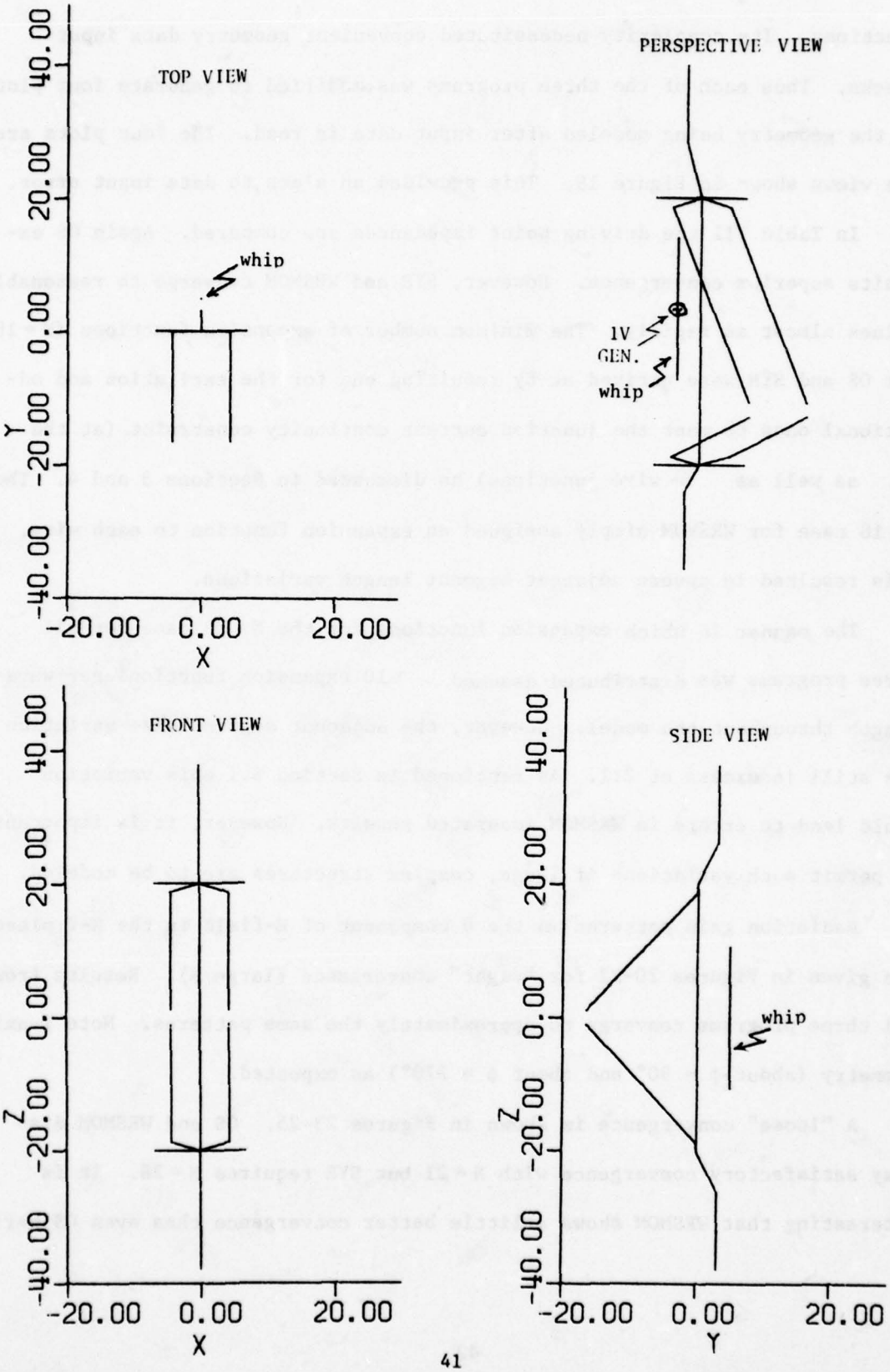

Figure 19. Three principal plane projections and a perspective of whip-excited fan model. All dimensions in meters. Excitation (center of whip) is shown in the perspective. Wire radius (all wires) = 0.01m. Frequency = 6.0 MHz.

junctions. Its complexity necessitated convenient geometry data input checks. Thus each of the three programs was modified to generate four plots of the geometry being modeled after input data is read. The four plots are the views shown in Figure 19. This provided an alert to data input error.

In Table III the driving point impedances are compared. Again OS exhibits superior convergence. However, SYR and WRSMOM converge to reasonable values almost as rapidly. The minimum number of expansion functions (N = 18) for OS and SYR were arrived at by requiring one for the excitation and additional ones to meet the junction current continuity constraint (at the 2- as well as 6- wire junctions) as discussed in Sections 3 and 4. The N = 18 case for WRSMOM simply assigned an expansion function to each wire. This resulted in severe adjacent segment length variations.

The manner in which expansion functions for the N = 80 case for all three programs was distributed assumed $\sim$10 expansion functions per wavelength throughout the model. However, the adjacent segment size variation was still in excess of 2:1. As mentioned in Section 6.1 this variation could lead to errors in WRSMOM generated results. However, it is important to permit such variations if large, complex structures are to be modeled.

Radiation gain patterns for the θ component of $\underset{\sim}{E}$-field in the X-Y plane are given in Figures 20-22 for "tight" convergence (large N). Results from all three programs converge to approximately the same patterns. Note Y-axis symmetry (about $\phi = 90°$ and about $\phi = 270°$) as expected.

A "loose" convergence is shown in Figures 23-25. OS and WRSMOM display satisfactory convergence with N = 21 but SYR requires N = 28. It is interesting that WRSMOM shows a little better convergence than even OS here.

TABLE III

Driving Point Impedance for Whip Excited Fan

No. of Expansion Functions (N)	Program		
	OS	SYR	WRSMOM
80	48.2-j122.0	47.3-j129.0	46.7-j127.6
18	32.1-j125.0	24.8-j219.0	23.4-j42.1
21	45.9-j122.0	33.5-j159.0	42.4-j114.8
22	48.2-j122.0	31.9-j157.0	39.5-j113.3
24	48.2-j122.0	30.4-j155.0	39.6-j113.3
28	48.2-j122.0	41.8-j150.0	42.1-j113.2
52	47.7-j123.0	45.6-j138.0	45.3-j124.8
68	48.1-j123.0	46.7-j132.0	45.7-j127.4

Dashed line underlines impedances which first fall within convergence criteria discussed in Section 5.

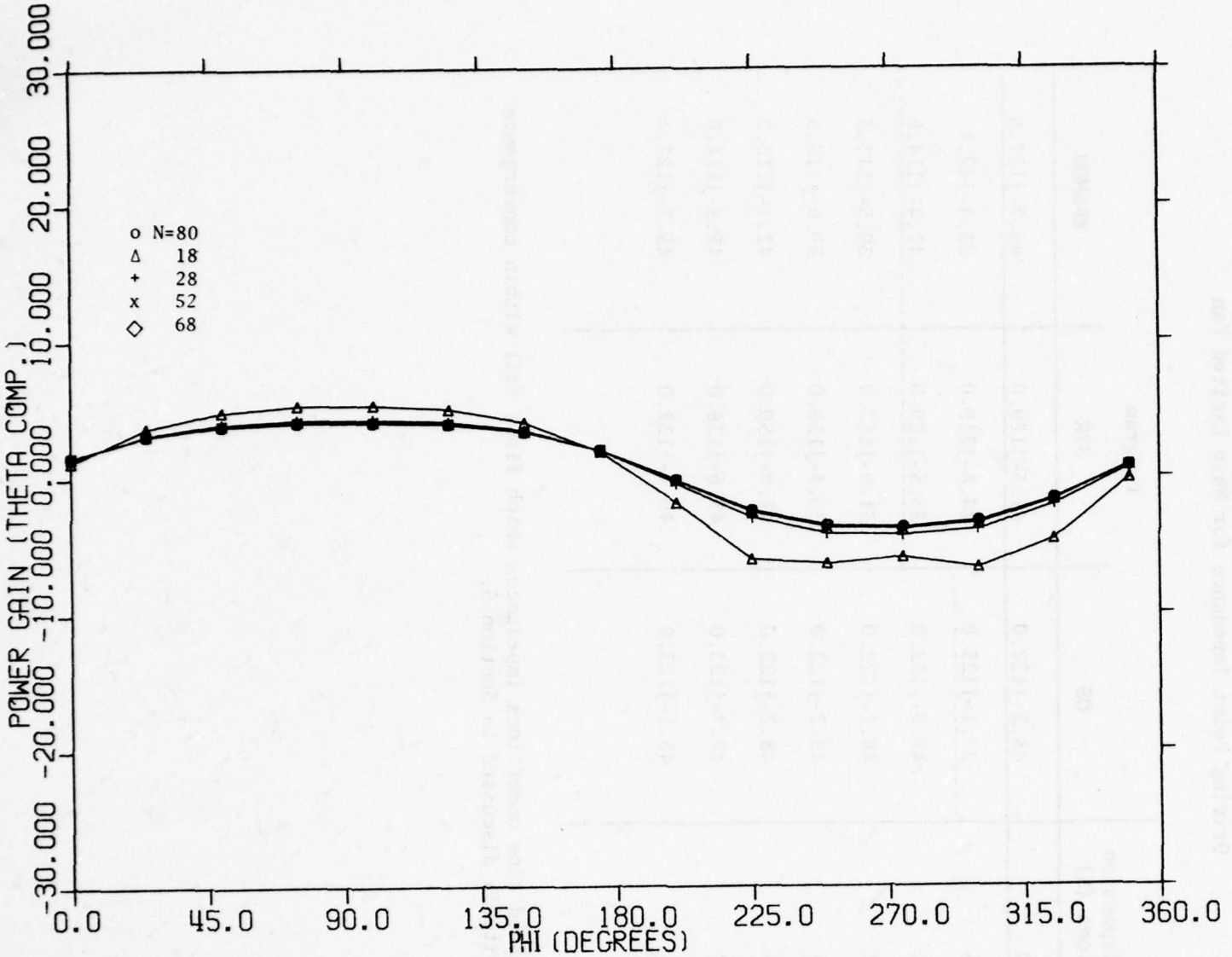

Figure 20. Radiation gain pattern (θ-component of E-field) convergence (tight) for OS applied to whip-excited twin fan.

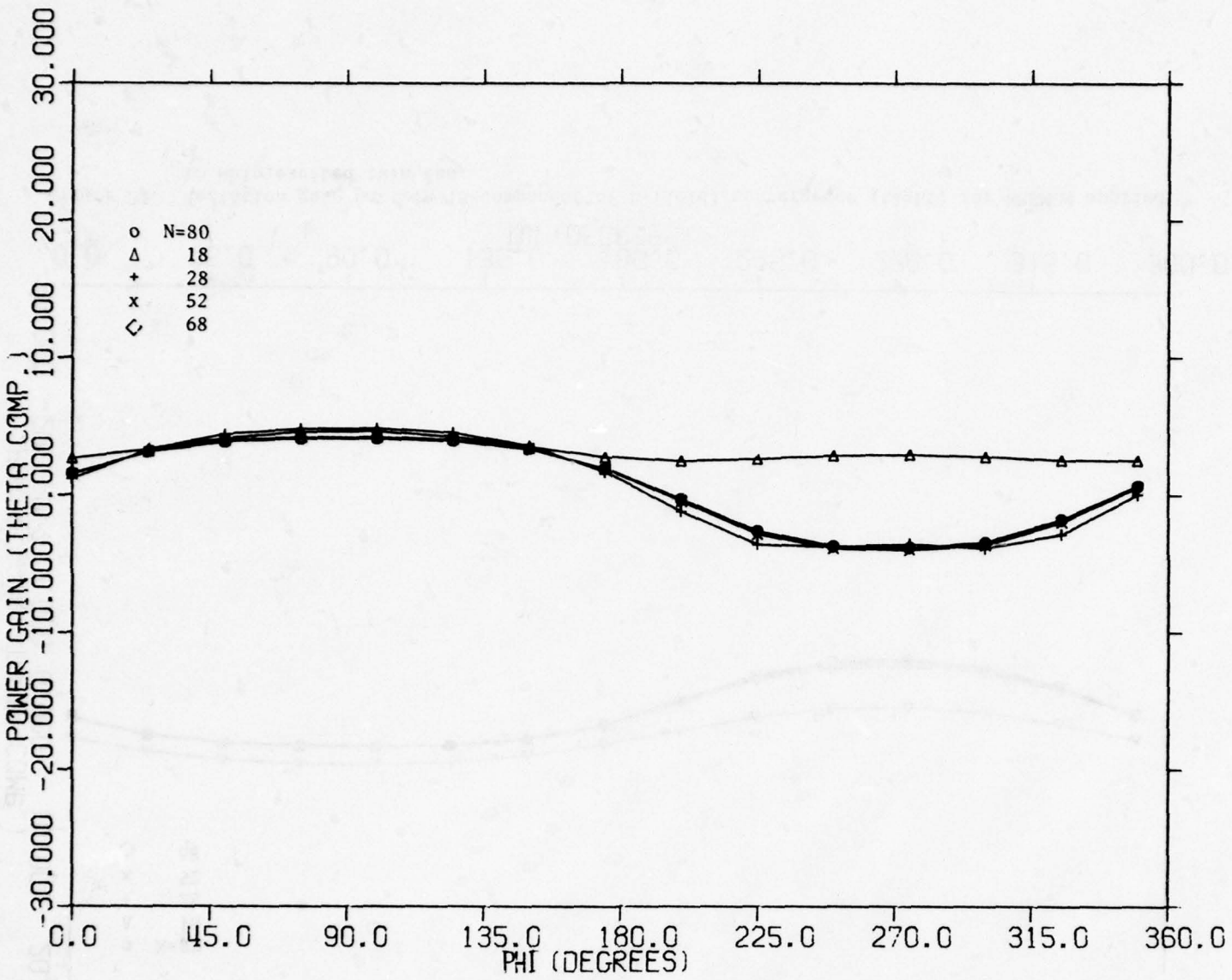

Figure 21. Radiation gain pattern (θ-component of E-field) convergence (tight) for SYR applied to whip-excited twin fan.

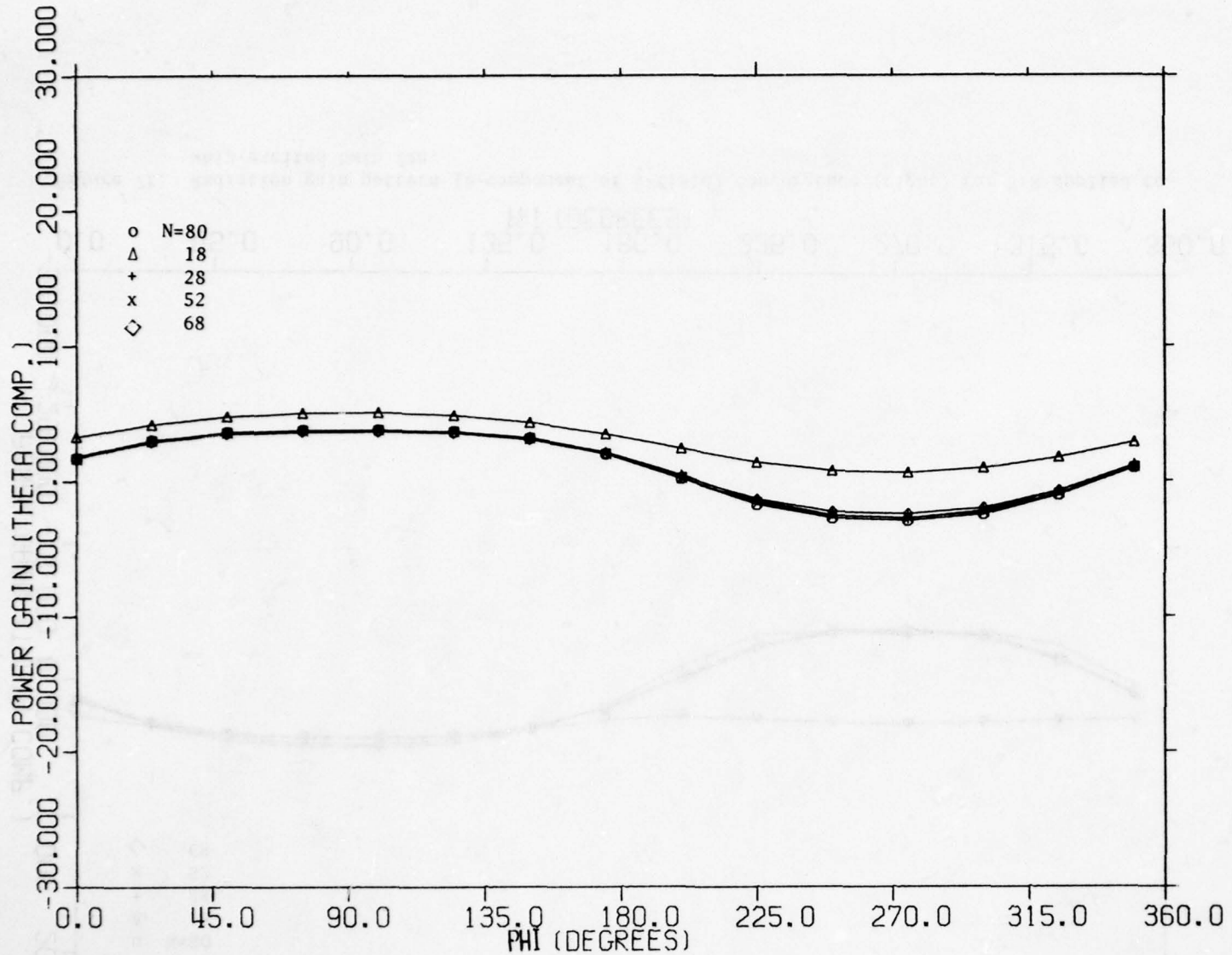

Figure 22. Radiation gain pattern (θ-component of E-field) convergence (tight) for WRSMOM applied to whip-excited twin fan.

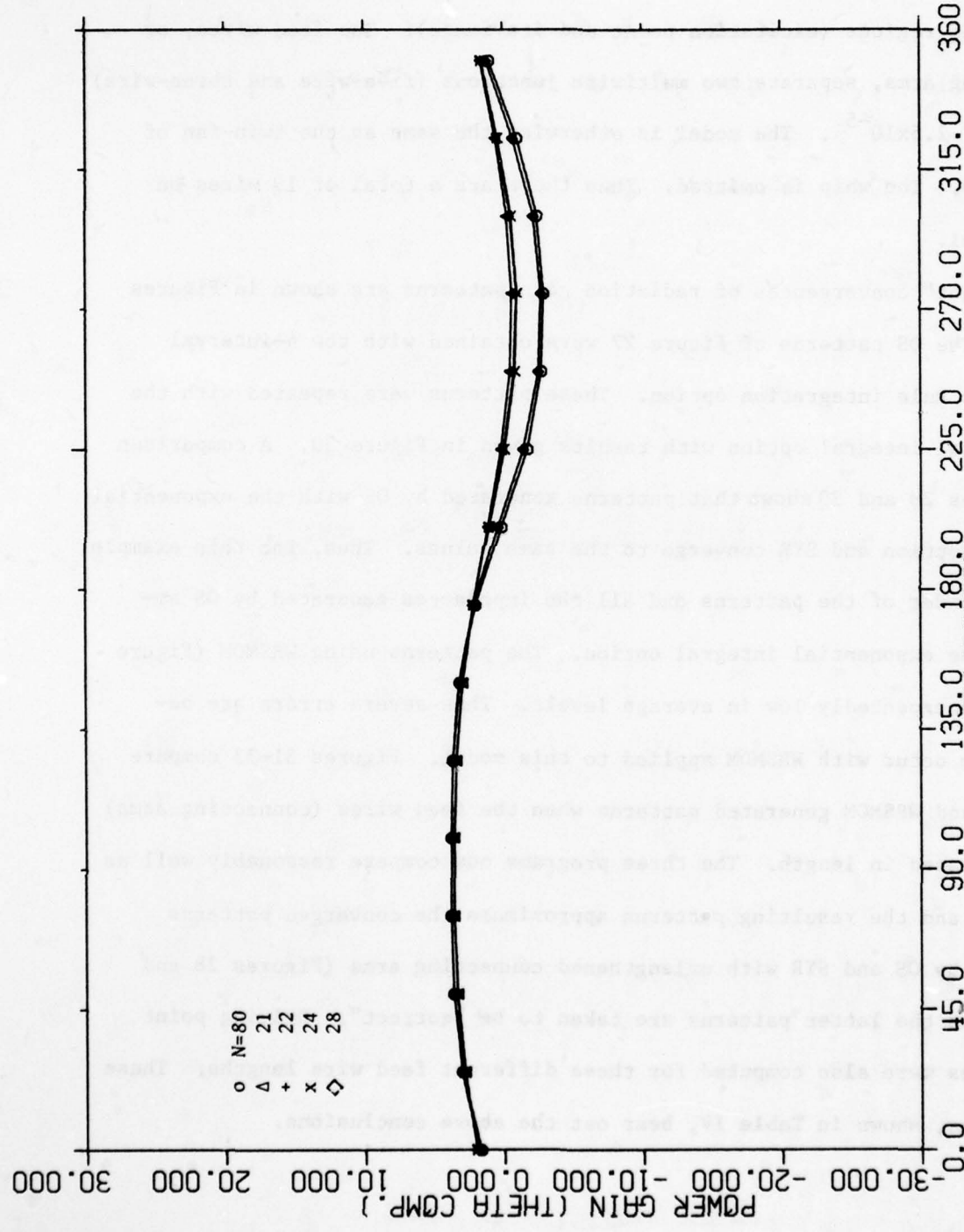

Figure 25. Radiation gain pattern (θ-component of $\underset{\sim}{E}$-field) convergence (loose) for WRSMOM applied to whip-excited twin fan.

B. Self-excited twin fan

This example provides the severest test for the three programs. This is readily apparent in Figure 26 which depicts blow-ups of the complicated feed regions (excitation point and its image). The feed wires, or connecting arms, separate two multiwire junctions (five-wire and three-wire) by only $\sim 2.5 \times 10^{-5}\lambda$. The model is otherwise the same as the twin-fan of Figure 19. The whip is omitted. Thus there are a total of 19 wires on this model.

"Tight" convergences of radiation gain patterns are shown in Figures 27-30. The OS patterns of Figure 27 were obtained with the 4-interval Simpson's Rule integration option. These patterns were repeated with the exponential integral option with results given in Figure 30. A comparison of Figures 28 and 30 shows that patterns generated by OS with the exponential integral option and SYR converge to the same values. Thus, for this example, the remainder of the patterns and all the impedances generated by OS employed the exponential integral option. The patterns using WRSMOM (Figure 29) are unexpectedly low in average levels. Thus severe errors are believed to occur with WRSMOM applied to this model. Figures 31-33 compare OS, SYR and WRSMOM generated patterns when the feed wires (connecting arms) are increased in length. The three programs now compare reasonably well as expected and the resulting patterns approximate the converged patterns computed by OS and SYR with unlengthened connecting arms (Figures 28 and 30). Thus the latter patterns are taken to be "correct". Driving point impedances were also computed for these different feed wire lengths. These impedances, shown in Table IV, bear out the above conclusions.

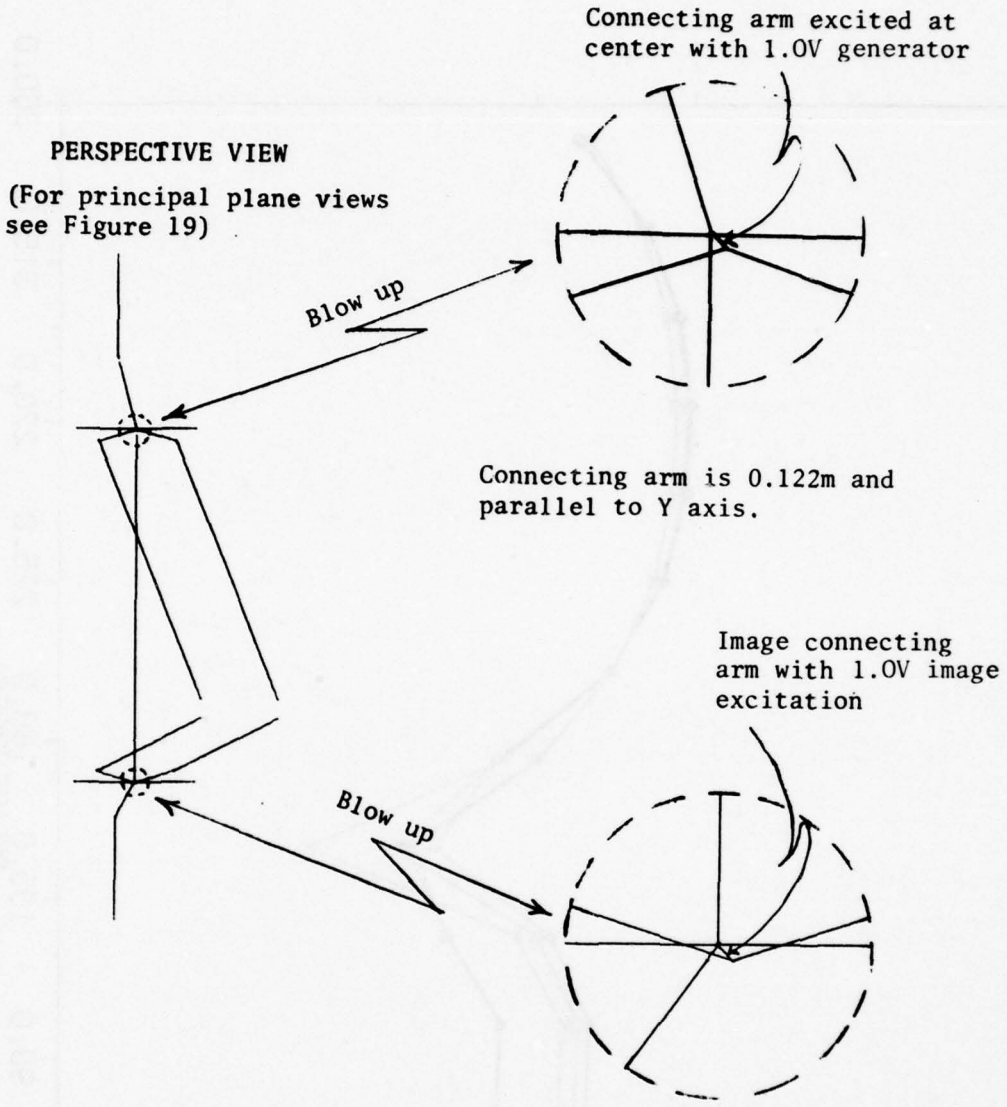

Figure 26. Perspective of self-excited twin fan model with blow-ups of junctions. Fan model same as in Figure 19 with the addition of the excited "connecting arms" at the junctions. Frequency=6.0 MHz.

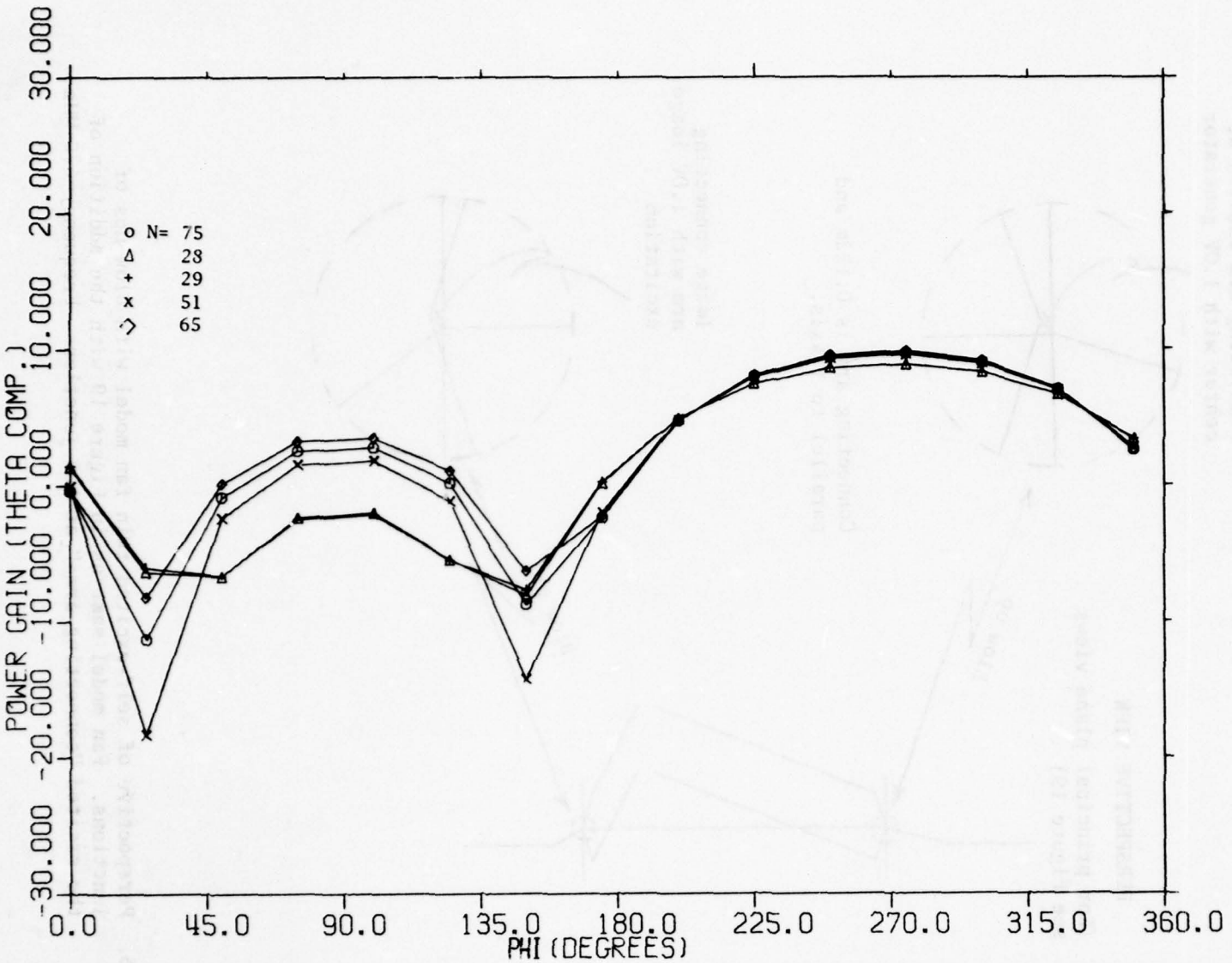

Figure 27. Radiation gain pattern (θ-component of $\tilde{E}$-field) convergence (tight) for OS applied to self-excited twin fan. (Four-interval Simpson's rule integration.)

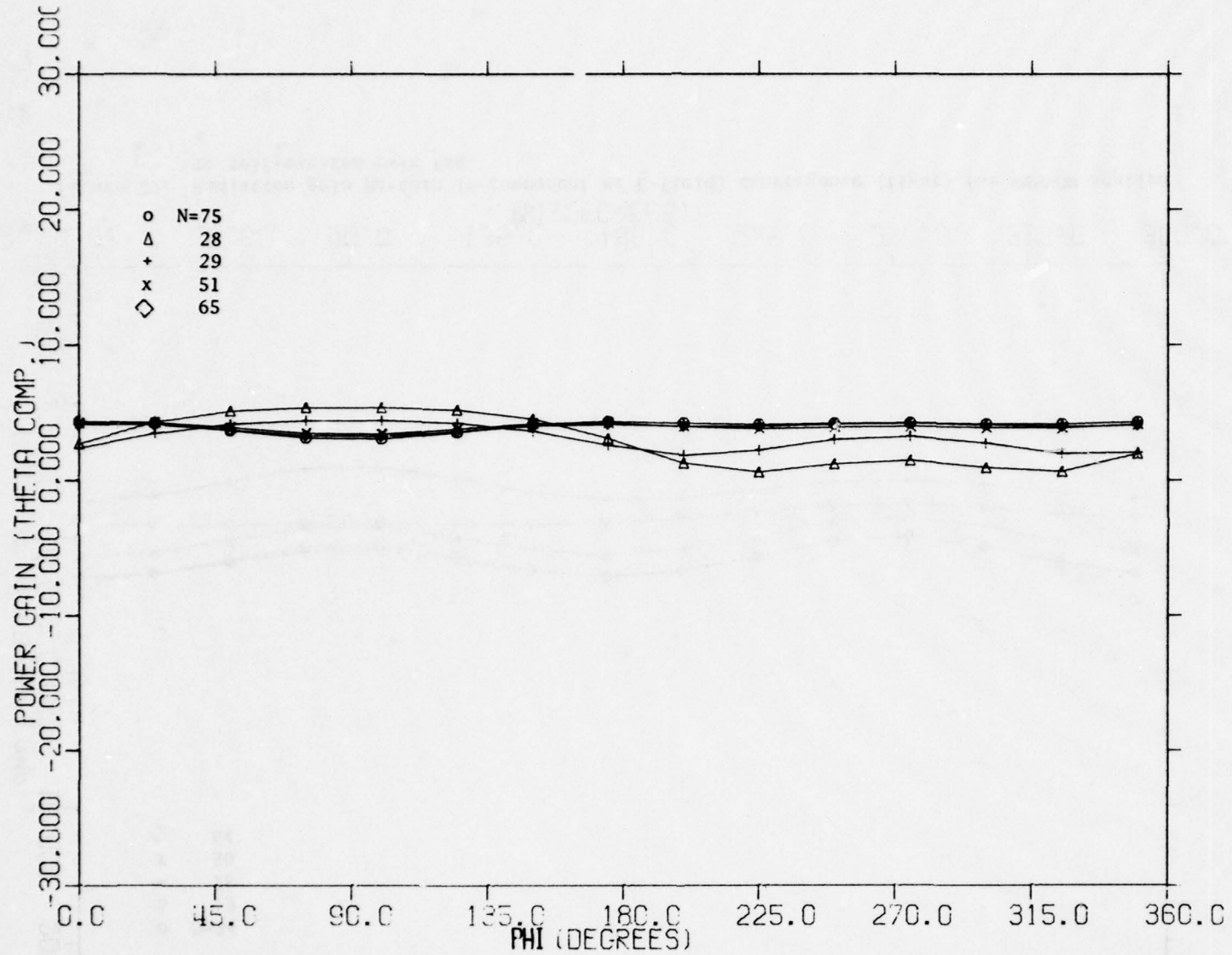

Figure 28. Radiation gain pattern (θ-component of $\underline{E}$-field) convergence (tight) for SYR applied to self-excited twin fan.)

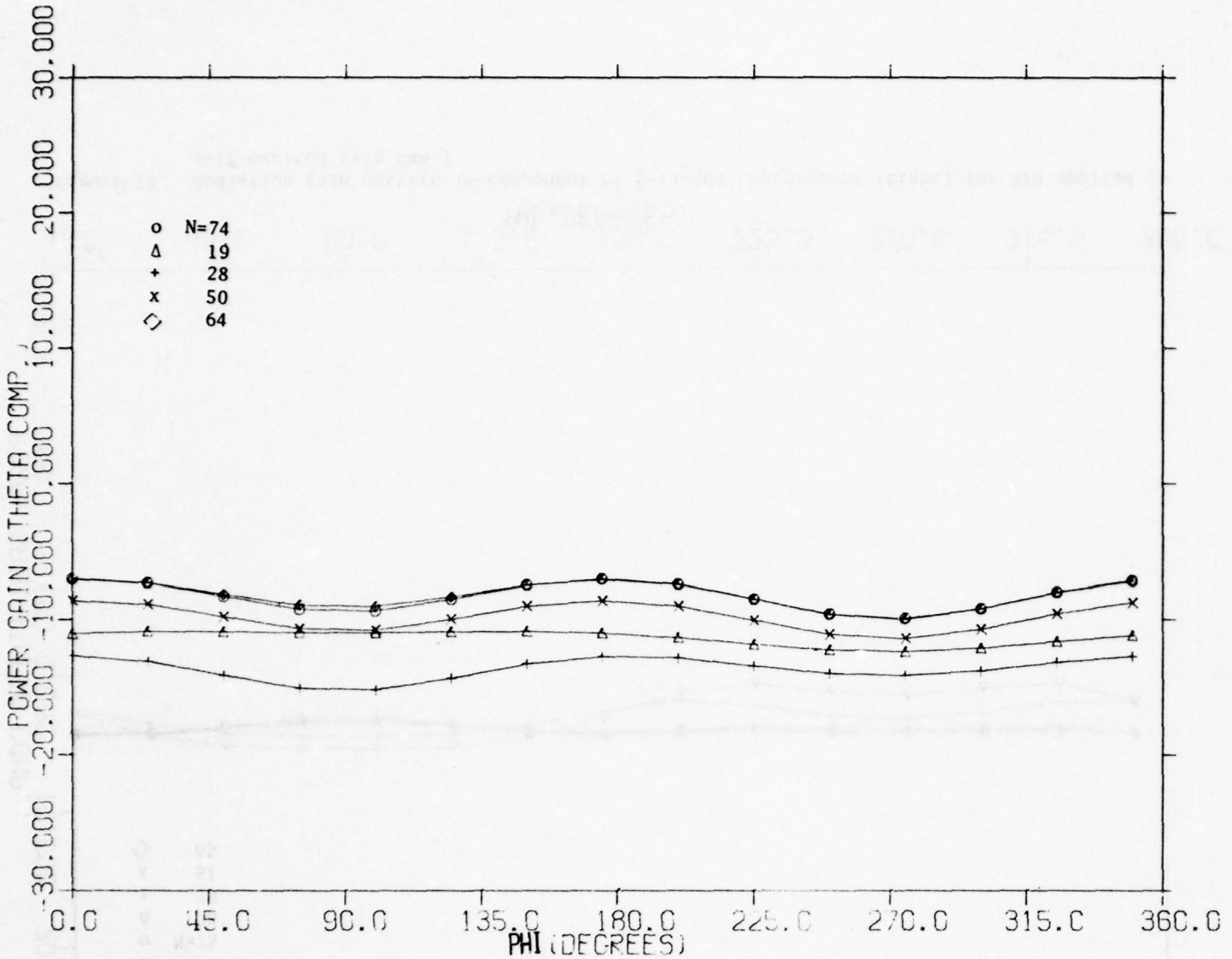

Figure 29. Radiation gain pattern (θ-component of E-field) convergence (tight) for WRSMOM applied to self-excited twin fan.

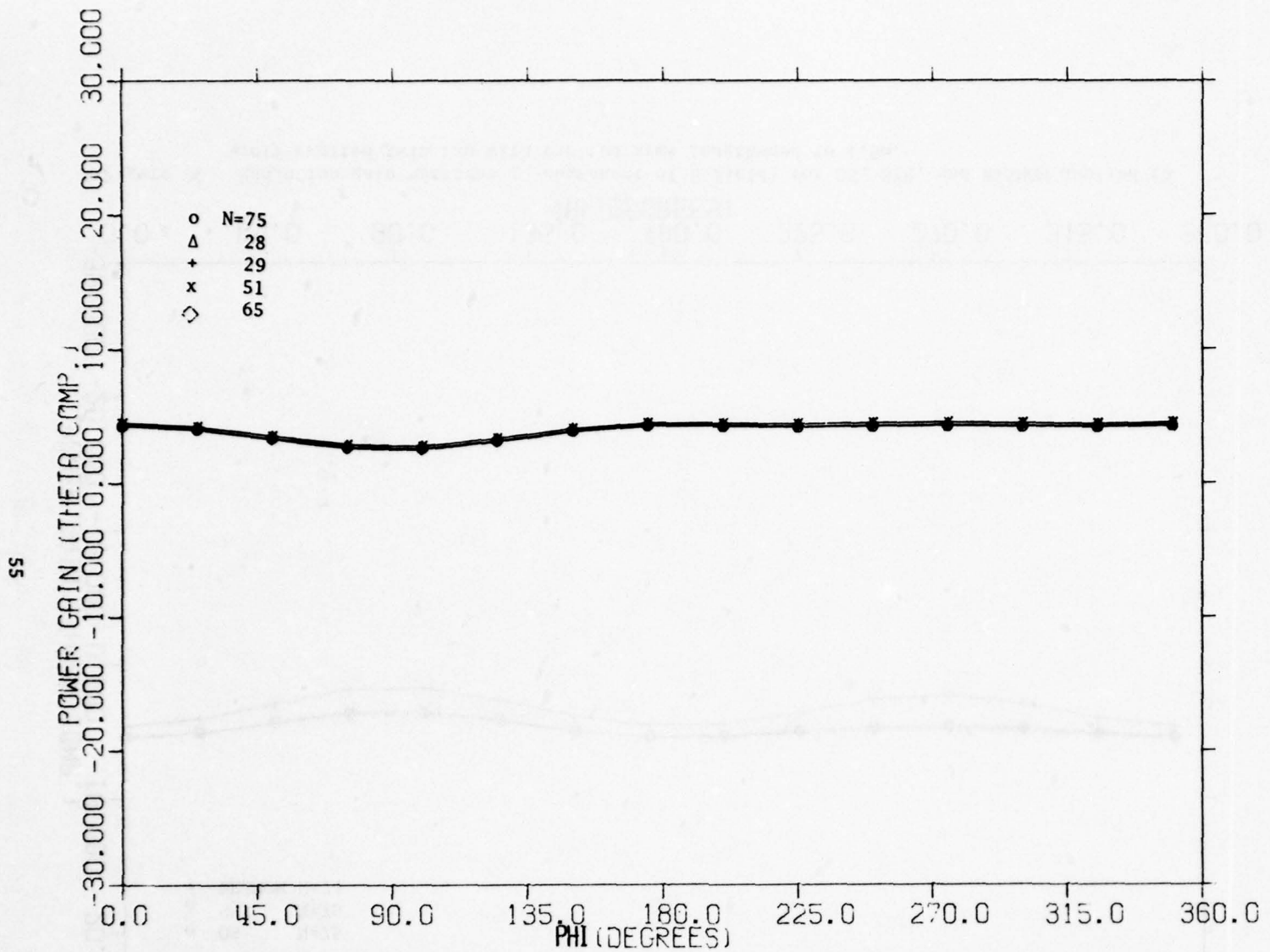

Figure 30. Radiation gain pattern (θ-component of E-field) convergence (tight) for OS applied to self-excited twin fan. (Exponential integral form.)

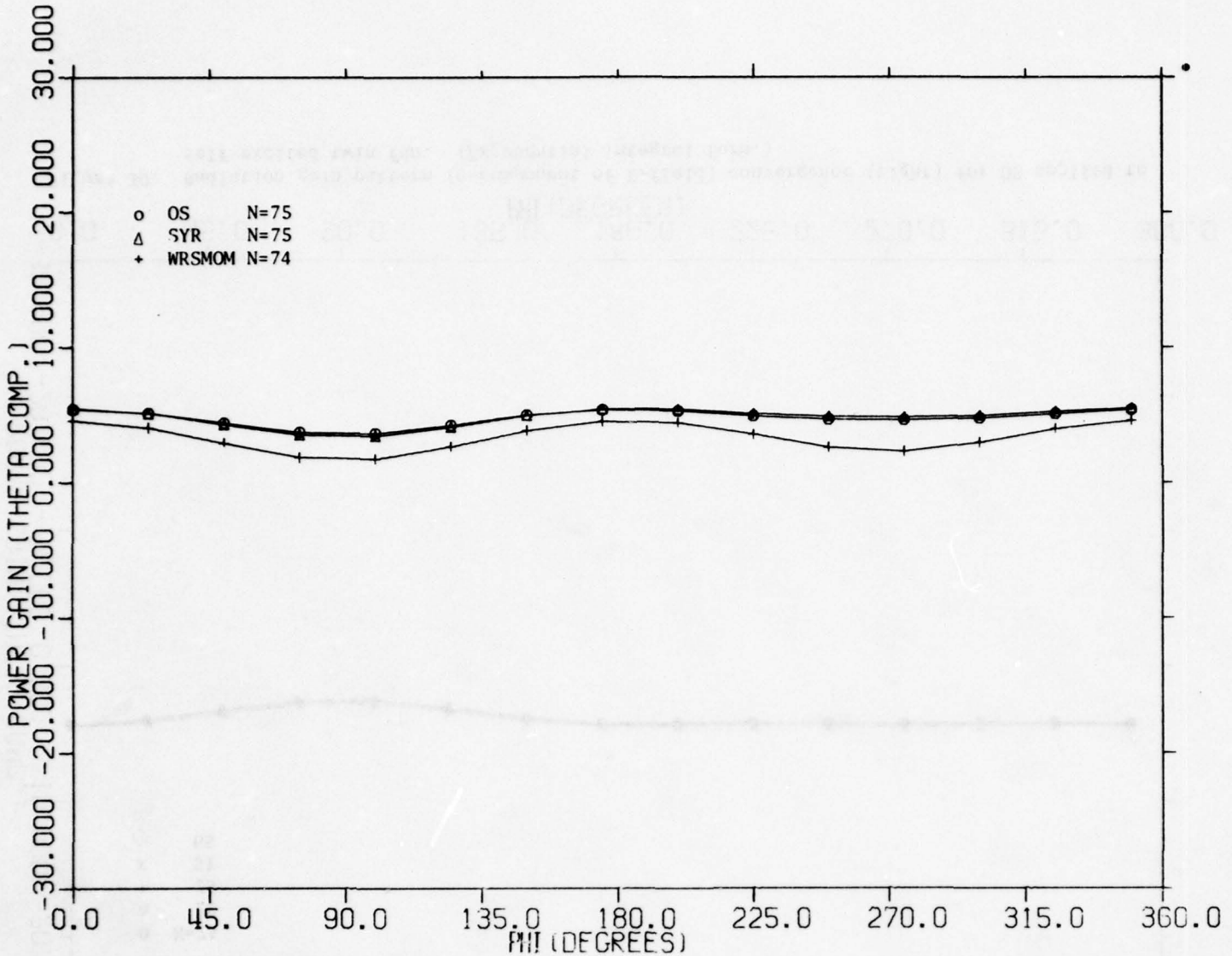

Figure 31. Radiation gain patterns (θ-component of E-field) for OS, SYR, and WRSMOM applied to self-excited twin fan with excited arms lengthened to 1.5m.

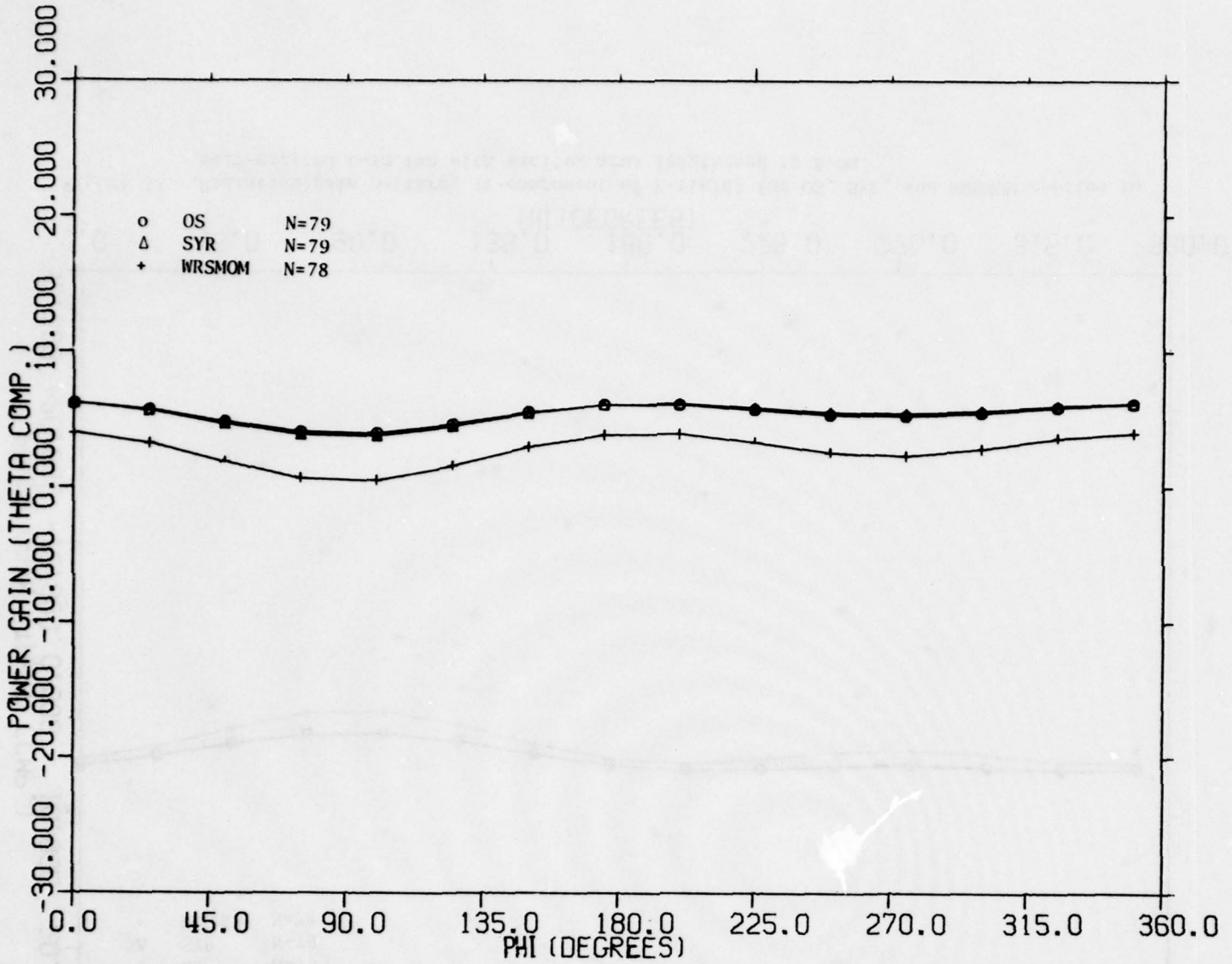

Figure 32. Radiation gain patterns (θ-component of $\underset{\sim}{E}$-field) for OS, SYR, and WRSMOM applied to self-excited twin fan with excited arms lengthened to 3.0m.

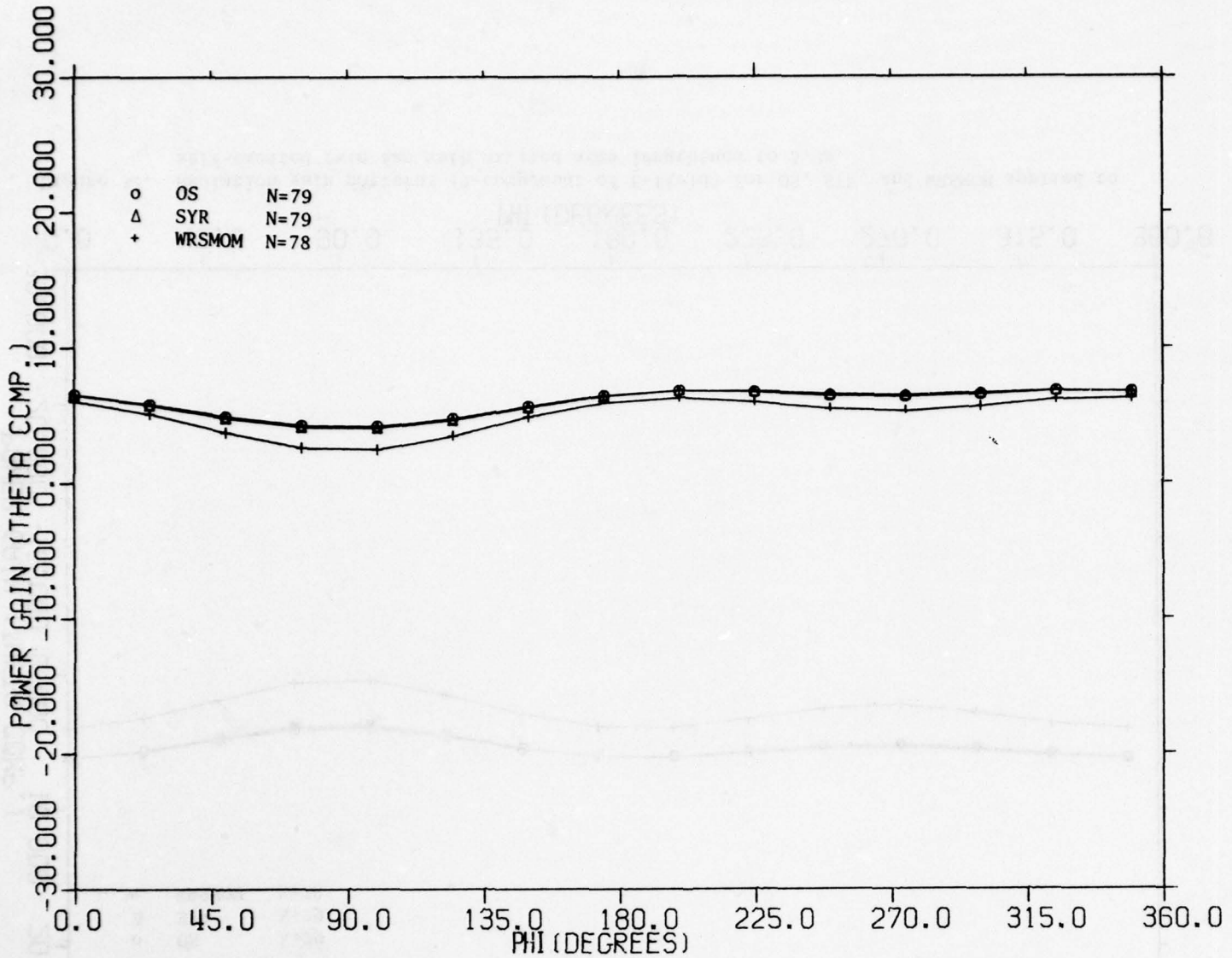

Figure 33. Radiation gain patterns (θ-component of E-field) for OS, SYR, and WRSMOM applied to self-excited twin fan with excited arms lengthened to 6.0m.

TABLE IV

Fan Impedance for Different Excitation Arm Lengths

Excitation Arm Length (λ)	No. of Exp. Fns.*	Program		
		OS	SYR	WRSMOM
2.44×10^{-3}	75	49.4-j206.3	52.2-j211.7	303.1-j2,915.0
0.03	75	61.1-j207.4	67.5-j215.5	44.5-j306.1
0.06	79	69.3-j182.2	77.0-j195.6	67.2-j384.3
0.12	79	80.4-j93.2	88.7-j109.5	50.7-j105.7

* For WRSMOM subtract 1 from these numbers.

"Loosely" converging patterns are shown in Figures 34-36. The convergence for OS is a bit superior to that for SYR in that N = 27 provides acceptable results for OS (Figure 34) and N = 29 for SYR (Figure 28).. Although the WRSMOM convergence is excellent (Figure 36), there is, as discussed above, considerable doubt as to its accuracy.

The convergence for driving point impedance is demonstrated in Table V. Both OS and SYR require the same N to achieve acceptable results.

The difficulty with WRSMOM for this example and the need for the more time consuming exponential integral option in OS can probably be alleviated by modeling the junction differently. For example the connecting arms between junctions can be removed by "passing the source through the junctions" such that Kirchoff's Voltage Law remains satisfied [Burke 1976]. Since two junctions are involved, the equivalent representation is not unique. One representation is shown in Figure 37. Here 1/2 the source is passed through each junction and the short connecting arm is then eliminated. The driving point impedance can now be approximated by dividing the algebraic sum of the currents entering the junction from points E and F into 1.0V.

6.3 Computer Run Time

The matrix fill ([Z] computation) time is proportional to N^2 and the simultaneous equation solution time is proportional to N^3. Thus the computer cpu time T in seconds for solving a moment method problem is given by

$$T \simeq AN^2 + BN^3$$

for reasonably large values of N, e.g. N > 40. The coefficients A and B for the three programs considered are given below. Values for the Honeywell

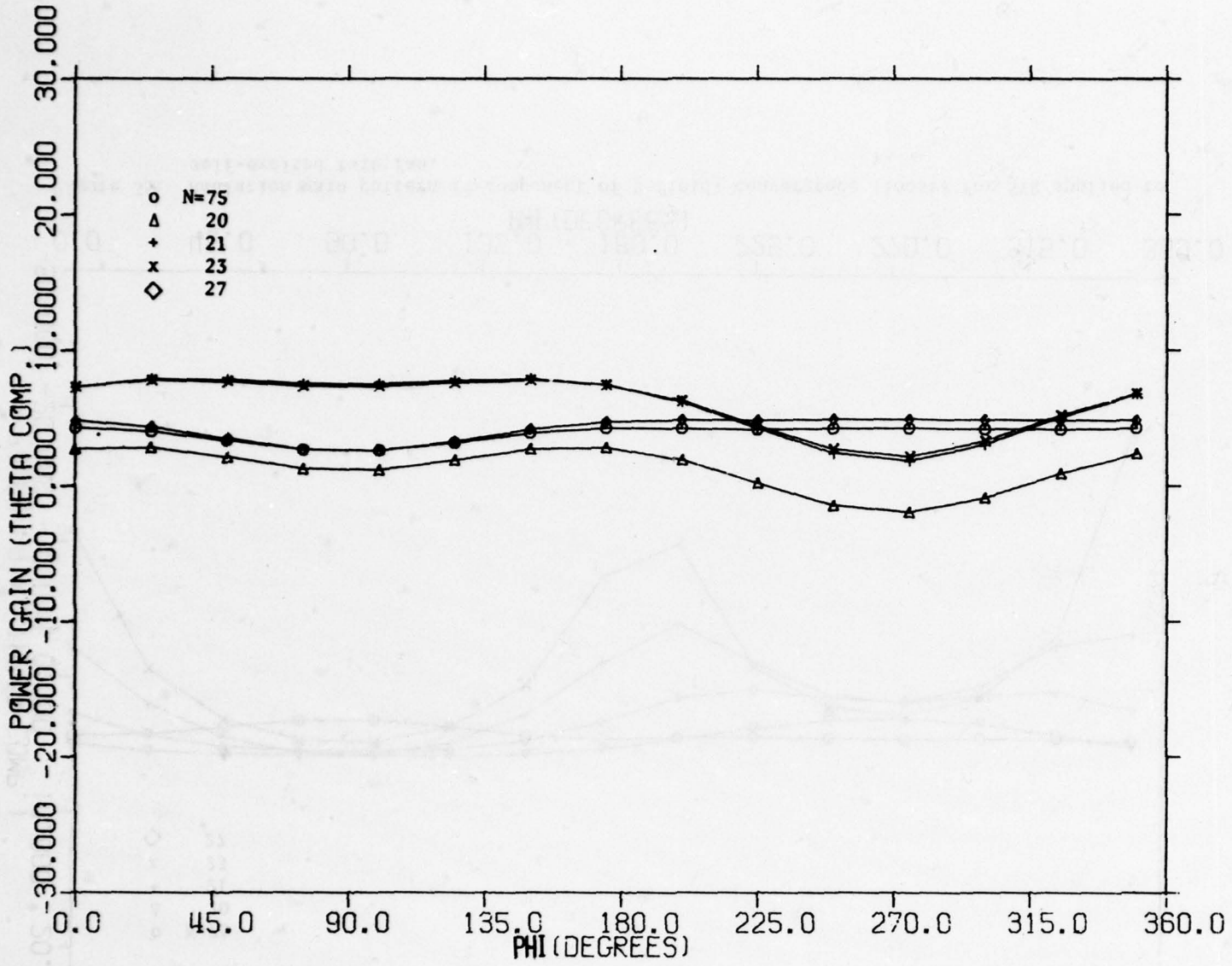

Figure 34. Radiation gain pattern (θ-component of E-field) convergence (loose) for OS applied to self-excited twin fan. (Exponential integral form).

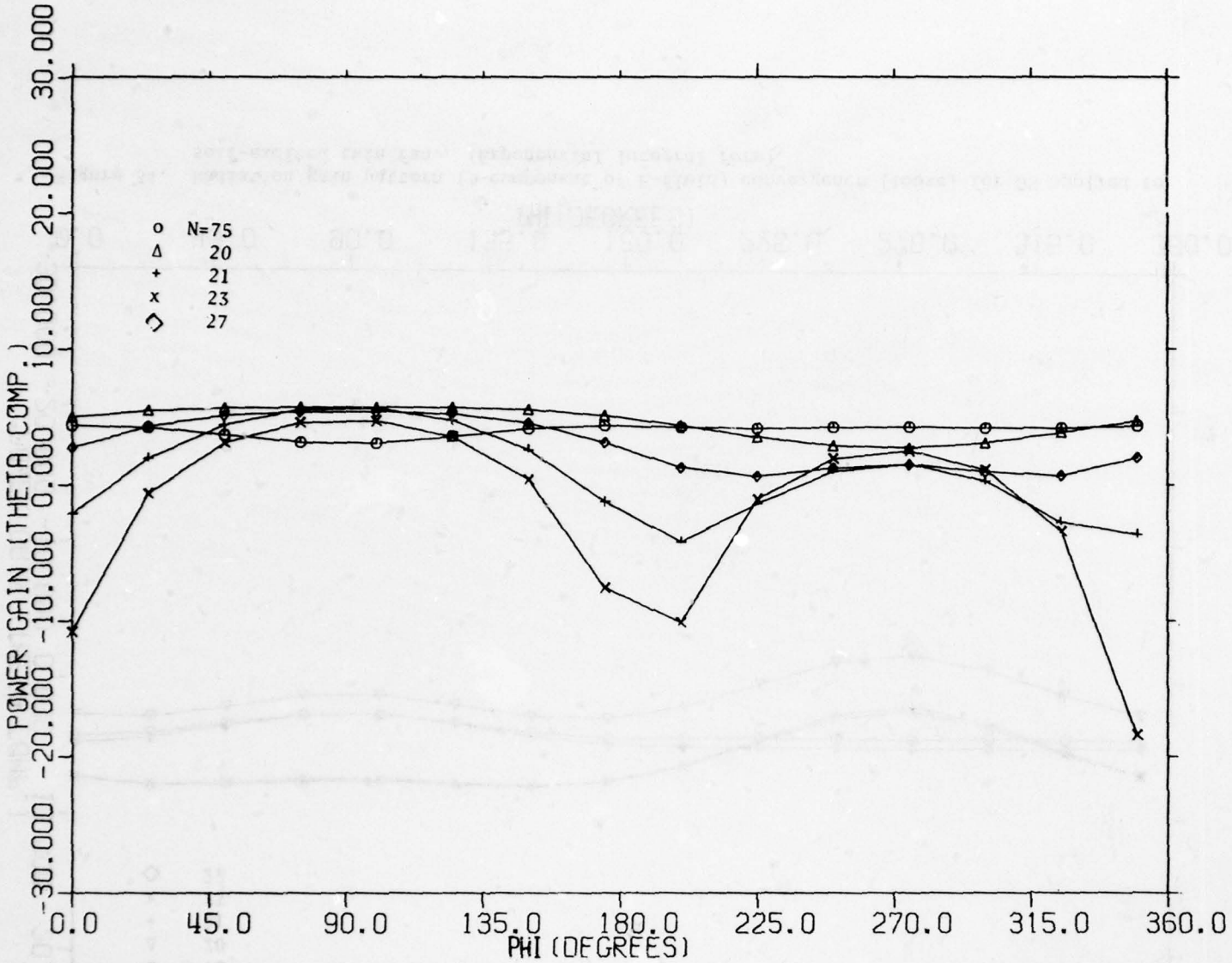

Figure 35. Radiation gain pattern (θ-component of E-field) convergence (loose) for SYR applied to self-excited twin fan.

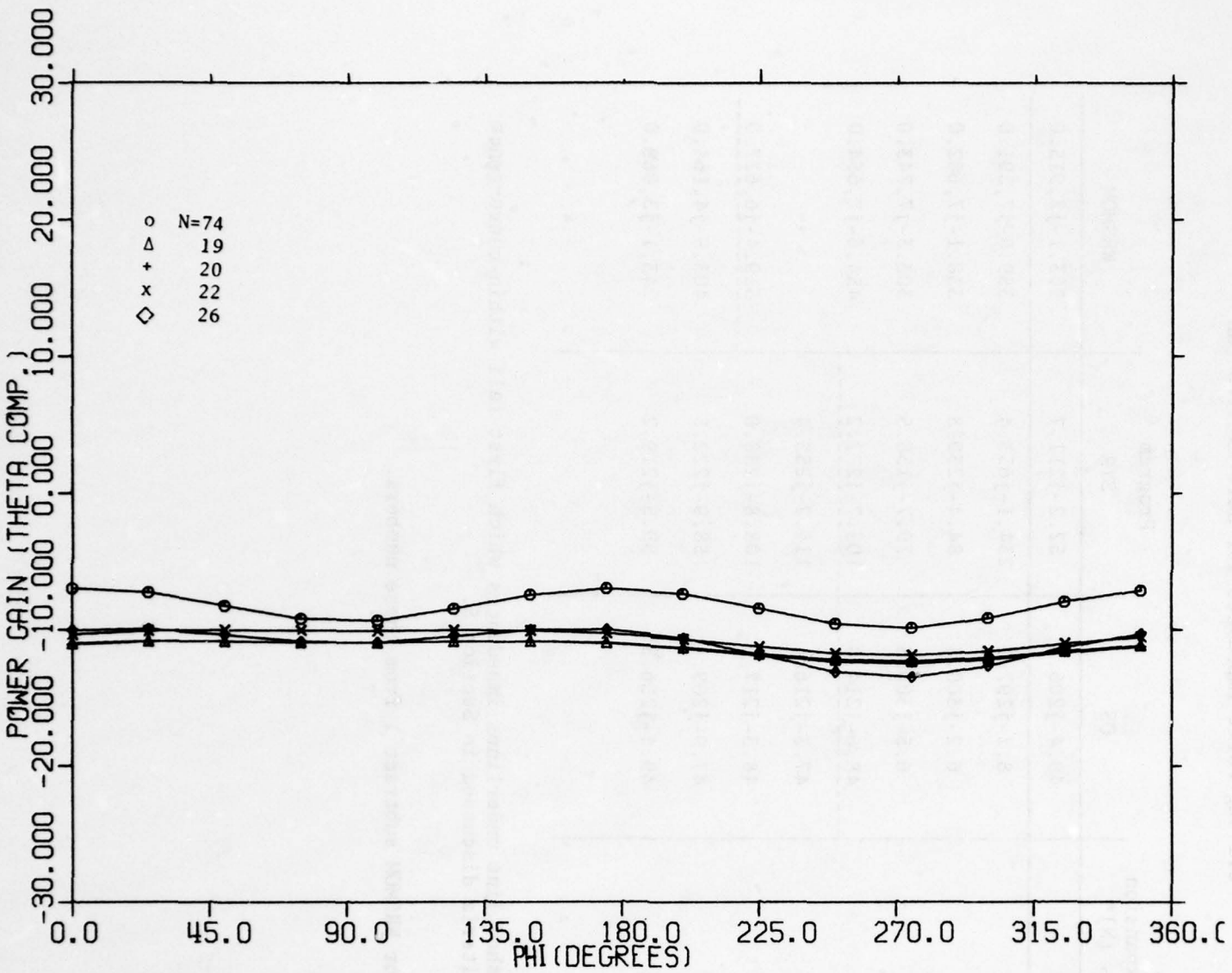

Figure 36. Radiation gain pattern (θ-component of E-field) convergence (loose) for WRSMOM applied to self-excited twin fan.

TABLE V

Driving Point Impedance for Self Excited Fan

No. of Expansion Functions (N)*	Program		
	OS	SYR	WRSMOM
75	49.4-j206.3	52.2-j211.7	303.1-j2,915.0
20	8.2-j297.1	234.1-j653.4	359.8-j7,591.0
21	6.2-j300.3	84.4-j239.8	338.1-j7,682.0
23	6.5-j300.3	79.7-j158.5	303.3-j7,743.0
27	48.6-j214.8	103.7-j272.2	454.6-j7,664.0
28	47.3-j216.4	114.2-j253.4	--
29	48.3-j217.3	108.8-j238.0	519.4-j6,627.0
51	47.9-j209.4	58.9-j222.5	403.9-j4,164.0
65	49.4-j206.5	59.5-j219.2	243.1-j3,068.0

Dashed line underlines impedances which first fall within convergence criteria discussed in Section 5.

*For WRSMOM subtract 1 from these numbers.

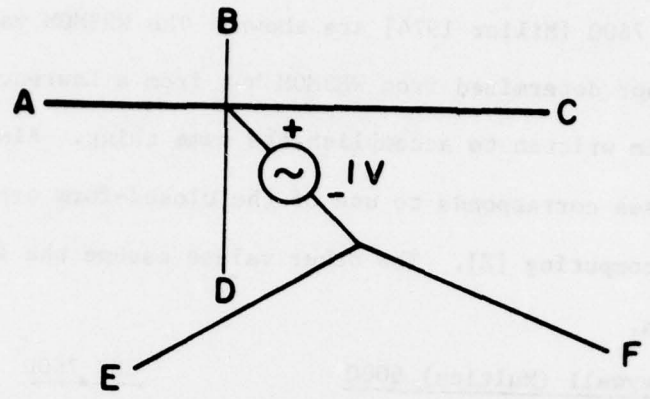

(a)

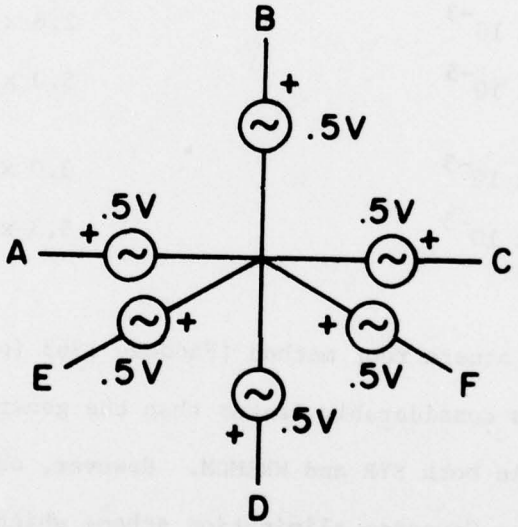

(b)

Figure 37. (a) Excited complex junction.
(b) Equivalent source representation.

(Multics) 6000 series system, the computer used throughout this work, and also for the CDC 7600 [Miller 1974] are shown. The WRSMOM values for the CDC system were not determined from WRSMOM but from a Lawrence Livermore Laboratory program written to accomplish the same thing. Also the OS value of A in parentheses corresponds to use of the closed-form exponential integral option for computing [Z]. The other values assume the 4-interval Simpson's Rule option.

		Honeywell (Multics) 6000	CDC 7600
OS	A	9.36×10^{-3} (4.54×10^{-2})	3.5×10^{-4}
	B	1.66×10^{-5}	1.07×10^{-6}
SYR	A	5.81×10^{-3}	2.6×10^{-4}
	B	9.18×10^{-5}	5.0×10^{-6}
WRSMOM	A	9.09×10^{-3}	3.0×10^{-4}
	B	9.18×10^{-5}	5.3×10^{-6}

OS employs the square root method [Faddeev 1963 (pp.144-147)] for solving (7). This is considerably faster than the general matrix inversion method incorporated in both SYR and WRSMOM. However, one can easily fit to either SYR or WRSMOM a Gaussian elimination scheme which simply solves (7). This would reduce their B values by about 1/3. Also SYR is approximately symmetric. Thus incorporation of the square root method in SYR might be feasible. This would further reduce B (and also lower A) for SYR.

For equal N the matrix fill time for SYR is smaller than for OS. This is especially true if the latter is run with the accurate but slow exponential integral option. SYR is also quicker than WRSMOM for matrix fill.

This is surprising since a Galerkin-triangle moment method is more complicated than pulse expansion-impulse weighting. However, the timing difference could be attributed to differences in programming efficiency.

Note that matrix fill is the dominating contributor to computer run time for N less than $\sim$100.

7. CONCLUSIONS

Three typical thin-wire moment method computer programs were compared. Two, OS and SYR, are basically Galerkin with sinusoids and triangles respectively. The third WRSMOM employs pulse expansion and impulse testing. These programs were applied to four thin-wire antenna examples, two simple and two complex. The parameters computed were driving point impedance and far-field radiation pattern. The principal variable was the number of expansion functions N. The program generally requiring least N to achieve fair ($\sim$3dB) agreement with converged parameter values was considered superior. Thus the main purpose was to determine if a "best" computer program exists given "coarse" accuracy as acceptable in predicting pattern and impedance for complex wire models.

The two simple models (straight, resonant wire and three-wire junction) were studied to gain confidence in the programs and evaluation method. For these examples OS was decidedly superior in computing driving-point impedances and all programs exhibited adequate pattern convergence with SYR lagging a bit.

The two complex wire models were (a) an eighteen wire "whip-excited twin fan" (Figure 19), and (b) a nineteen-wire "self-excited twin fan"

(Figure 26). The latter is a relatively simple model of a very complex shipboard antenna. The model includes an image to simulate a perfectly conducting, flat ground.

The whip-excited twin fan model is representative of large complex structures. It includes junctions formed by as many as six intersecting wires. However, the excited wire is relatively uncomplicated. For this example all three programs demonstrated satisfactory impedance convergence with OS having a slight edge. The OS and WRSMOM pattern convergences were about equal and superior to that of SYR.

The self-excited twin fan is similar to the whip-excited model except that the excited wires are now on the twin fan part of the model. These wires are quite short, $\sim 0.0025\lambda$, and they separate two multiple-wire junctions. First the programs were applied directly to this severe example. Only SYR provided reasonable results. The OS runs were repeated with an optional time-consuming matrix element computation in terms of exponential integrals. This resulted in convergence of impedance and pattern similar to that for SYR. The WRSMOM results were exceptionally poor. However, this difficulty can often be eliminated by altering the model. An example of one such "equivalent" model was discussed in Section 6.2.

The often cited drawback of WRSMOM of inadequate junction treatment was not evident in these examples. A more plausible culprit is large adjacent segment length variations. This is suggested in Table IV and Figures 31-33 where lengthening the feed wire on the self-excited twin fan model corrected the WRSMOM results. However, even adjacent segment length variations of

$\sim$ 2:1 brought reasonable results.

One drawback of OS is an inability to analyze models with wires of differing radii. Thus each example exhibited a uniform wire radius. It was noted, however, that this constraint may prove minor in the process of reducing a highly complicated structure to a viable wire model.

The [Z] computation time for SYR was about half that for OS and even WRSMOM for the same N. Also for the same N the simultaneous equations (7) solution time for OS was about one-sixth that for SYR or WRSMOM. This is because SYR and WRSMOM employ the slow matrix inversion method. However, quicker subprograms to solve (7) can easily be incorporated in SYR and WRSMOM.

The overall conclusion is that for "coarse" accuracy in solving complex wire models by moment methods, most currently available programs are probably comparable. It is important, however, that a convergence test be performed for each example regardless of the program.

REFERENCES

(References are ordered alphabetically according to first appearing author's last name and by date for multiple papers by one author.)

1. T.E. Baldwin, Jr. and Richard Robertson, "Thin Wire Antenna Analysis Computer Codes Compared with Measured Data," RADC-TR-73-217, Method of Moments Applications, Volume V, Final Report, Rome Air Development Center, Air Force Systems Command, Griffiss Air Force Base, New York, July 1974, AD# 783897/2GI.

2. D. Buchanan, et. al., "Assessment of MOM Techniques for Shipboard Applications," phase report RADC-TR-77-14 for Rome Air Development Center, Air Force Systems Command, Griffiss AFB, New York under contract F30602-75-C-0121 with Syracuse University, January 1977, AD# B016694L.

3. G.J. Burke and A.J. Poggio, "Computer Analysis of the Bottom-Fed Fan Antenna," Report UCRL-52109, Lawrence Livermore Laboratory, University of California, Livermore, California, August 1976.

4. C.M. Butler, "Currents Induced on a Pair of Skew Crossed Wires," IEEE Trans. Antenna Propagat., Vol. AP-20, pp. 731-736, Nov. 1972.

5. C.M. Butler and D.R. Wilton, "analysis of Various Numerical Techniques Applied to Thin-Wire Scatterers," IEEE Trans. Antenna Propagat., Vol. AP-23, pp. 534-540, July 1975.

6. H.H. Chao and B.J. Strait, "Computer Programs for Radiation and Scattering by Arbitrary Configurations of Bent Wires," Scientific Report No. 7 on Contract F19628-68-C-0180, AFCRL-70-0374; Syracuse University, Syracuse, N.Y., Sept. 1970.

7. D.K. Faddeev and V.N. Faddeeva, Computational Methods of Linear Algebra, W.H. Freeman and Company, San Francisco, 1963.

8. R.F. Harrington, "Matrix Methods for Field Problems," Proceedings of the IEEE, Vol. 55, No. 2, pp. 136-149, February 1967.

9. R.F. Harrington, Field Computation by Moment Methods, The Macmillan Company, 1968.

10. R.F. Harrington, and J.R. Mautz, "Radiation and Scattering from Bodies of Revolution," Final Report, prepared for Air Force Cambridge Research Laboratories, Bedford, Mass., under Contract F19628-67-C-0233 with Syracuse University, Syracuse, N.Y. 13210, July 1969.

11. W.A. Imbriale and P.G. Ingerson, "On Numerical Convergence of Moment Solutions of Moderately Thick Wire Antennas Using Sinusoidal Basis Functions," IEEE Transactions on Antennas and Propagation, Vol. AP-21, pp. 363-366, May 1973.

12. E.C. Jordan, Electromagnetic Waves and Radiating Systems, Prentice-Hall, New York, 1950.

13. D.C. Kuo and B.J. Strait, "Improved Programs for Analysis of Radiation and Scattering by Configurations of Arbitrarily Bent Thin Wires," Scientific Report No. 15, Contract No. F19628-68-C-0180 with Air Force Cambridge Research Laboratories, Bedford, Massachusetts, January 1972. Or see instead, D.C. Kuo, H.H. Chao, J.R. Mautz, B.J. Strait and R.F. Harrington, "Analysis of Radiation and Scattering by Arbitrary Configurations of Thin Wires," (computer program description), IEEE Trans. on Antennas and Propagation, vol. AP-20, No. 6, pp. 814-815, Nov. 1972. See also, M.D. Tew, "Correction to WIRES Program," IEEE Trans. on Antennas and Propagation, Vol. AP-23, No. 3, pp. 450-451, May 1975. A program listing is available from NAPS as document 01798.

14. J.C. Logan, "A Comparison of Techniques for Treating Radiation and Scattering by Wire Configurations with Junctions," Report TR-73-10, Department of Electrical and Computer Engineering, Syracuse University, Syracuse, N.Y. 13210, August 1973.

15. J.R. Mautz and R.F. Harrington, "*H-Field, E-Field and Combined Field* Solutions for Bodies of Revolution," Interim Technical Report, RADC-TR-77-109, Rome Air Development Center, Griffiss Air Force Base, New York, March 1977, AD# A040379.

16. K.K. Mei, "On the Integral Equations of Thin Wire Antennas," IEEE Trans. Antennas Propagat., Vol. AP-13, pp. 374-378, May 1965.

17. E.K. Miller, et. al., "An Evaluation of Computer Programs Using Integral Equations for the Electromagnetic Analysis of Thin Wire Structures," Report UCRL-75566 Rev. 1, Lawrence Livermore Laboratory, University of California, Livermore, California, March 1974.

18. R. Mittra and W.L. Ko, "A Finite Difference Approach to the Wire Junction Problem," IEEE Trans. on Antennas and Propagation, Vol. AP-23, pp. 435-438, May 1975.

19. J.H. Richmond, "Computer Analysis of Three-Dimensional Wire Antennas," Technical Report 2708-4 for the Army Ballistic Research Laboratory under Contract No. DAAD 05-69-C-0031 with the Ohio State University ElectroScience Laboratory, Columbus, Ohio, December 1969.

20. J.H. Richmond, "Radiation and Scattering by Thin-Wire Structures in the Complex Frequency Domain," Report CR-2396 for the National Aeronautics and Space Administration, Washington, D.C. by The Ohio State University ElectroScience Laboratory, Columbus, Ohio, May 1974a.

21. J.H. Richmond, "Radiation and Scattering by Thin-Wire Structures in a Homogeneous Conducting Medium," (Computer program description), IEEE Trans. on Antennas and Propagation, Vol. AP-22, No. 2, p. 365, March 1974b. See also NAPS document 02223.

22. J.H. Richmond, "Computer Program for Thin-Wire Structures in a Homogeneous Conducting Medium," The Ohio State ElectroScience Laboratory, No Date.

23. H.A. Rogers, "An Evaluation of Thin-Wire-Theory Antenna Computer Programs for the Case of a Crossed-Dipole Scatterer," Master's Thesis, Naval Post Graduate School, June 1974.

24. J.R. Stewart, "Application of Optimization Theory to Electromagnetic Radiation and Scattering," Ph.D. dissertation, Syracuse University, Syracuse, N.Y., January 1974.

25. C.D. Taylor, "Electromagnetic Scattering from Arbitrary Configurations of Wires," IEEE Trans. on Antennas and Propagation, Vol. AP-17, pp. 662-663, September 1969.

26. G.A. Thiele, Chapter 2 of Computer Techniques for Electromagnetics, Edited by R. Mittra, Pergamon Press Ltd., 1973.

27. D.E. Warren, "Near Electric and Magnetic Fields of Wire Antennas," (Computer program description) Vol. AP-22, No. 2, p. 364, March 1974. See also NAPS document 02221. Or see instead: D.E. Warren, "A User Manual for Program WRSMOM," available from the author, Rome Air Development Center, Air Force Systems Command, Griffiss AFB, New York 13441.

28. D.E. Warren, private communication, 1976.

29. D.R. Wilton and C.M. Butler, "Efficient Numerical Techniques for Solving Pocklington's Equation and Their Relationships to Other Methods," IEEE Trans. on Antennas and Propagation, Vol. AP-24, pp. 83-86, January 1976.